

# **CONNECTIVITY AND RUNOFF DYNAMICS IN HETEROGENEOUS DRAINAGE BASINS**

A thesis submitted to the  
College of Graduate Studies and Research  
in Partial Fulfillment of the Requirements  
for the Degree of Master of Science  
in the Department of Geography and Planning  
(Centre for Hydrology)  
University of Saskatchewan  
Saskatoon, Canada

By: ROSS WILSON PHILLIPS

© Copyright R. W. Phillips, January, 2011.

All rights reserved.

## **PERMISSION TO USE**

In presenting this thesis in partial fulfilment of the requirements for a Postgraduate degree from the University of Saskatchewan, I agree that the Libraries of this University may make it freely available for inspection. I further agree that permission for copying of this thesis in any manner, in whole or in part, for scholarly purposes may be granted by the professors who supervised my thesis work or, in their absence, by the Head of the Department or the Dean of the College in which my thesis work was done. It is understood that any copying or publication or use of this thesis or parts thereof for financial gain shall not be allowed without my written permission. It is also understood that due recognition shall be given to me and to the University of Saskatchewan in any scholarly use which may be made of any material in my thesis.

Requests for permission to copy or to make other use of material in this thesis in whole or part should be addressed to:

Head of the Department of Geography and Planning  
University of Saskatchewan  
Saskatoon, Saskatchewan  
S7N 5C8 Canada

## **ACKNOWLEDGEMENTS**

This thesis is the result of the generous assistance provided by many colleagues, friends, and family. I would foremost like to thank my supervisors Dr. Chris Spence and Dr. John Pomeroy. Dr. Spence acted as a mentor and provided valuable feedback, guidance and perspective. Dr. Pomeroy provided invaluable perspective on how my research related to and benefited hydrology in general. It was an honour to have been able to work with them both. I am also much obliged to the other members of my supervisory committee: Dr. Xulin Guo of the College of Arts and Sciences, Dr. Charles Maule of the College of Engineering, and my external examiner Dr. Bing Si of the College of Agriculture and Bioresources. They all provided valuable feedback and advice that shaped my thought process and this thesis.

I would also like to thank those who aided in the completion of the field work associated with this project. Kirby Ebel and May Guan were excellent colleagues and company during the time we spent together at the Baker Creek Research Basin. Their work ethic in difficult circumstances and patience with my shortcomings was inspiring and admirable. Shawne Kokelj and Meg McCluskie of the Water Resources Division of Indian and Northern Affairs Canada Yellowknife and Newell Hedstrom of Environment Canada were also a great help in the field. Bob Reid provided unending support and hospitality when we were in Yellowknife, NT. The Yellowknife office of the Water Survey of Canada generously received our daily safety calls throughout the time spent at Baker Creek. Chris Spence, Bob Reid, Raoul Granger, and May Guan all provided access to supplementary data from Baker Creek.

This thesis wouldn't have been possible without the support of my peers at the University of Saskatchewan. I would like to thank all of my fellow students which made me smile and laugh, provided me with timely advice, and made the whole experience of graduate school enjoyable. May Guan deserves exceptional thanks for her advice and mentorship. I was also incredibly fortunate to have met and enjoyed the company of Nathalie, Matt, Nicole, Chris M., Chris D., Chad, Adam, Erin, Hawi, Lawrence and Allison.

This project would not have been possible without the generous financial support of several funding bodies: the Canadian Foundation for Climate and Atmospheric Sciences through the Improved Processes and Parameterization for Prediction in Cold Regions (IP3) Research Network, the Natural Sciences and Engineering Research Council through an Alexander Graham Bell Canadian Graduate Scholarship and Northern Research Internship, the U of S College of Graduate Studies and Research through a Dean's Scholarship, Indian and Northern Affairs Canada (INAC) through the Northern Scientific Training Program, the Water Resources Division of the Yellowknife office of INAC through their participation in the Northern Research Internship, the Garfield Weston Foundation through the Garfield Weston Award for Northern Research, the U of S Department of Geography and Planning through a J.H. Richards Graduate Award, Environment Canada, and the International Polar Year.

## ABSTRACT

A drainage basin's runoff response can be determined by the connectivity of generated runoff to the stream network and the connectivity of the downstream stream network. The connectivity of a drainage basin modulates its ability to produce streamflow and respond to precipitation events and is a function of the complex and variable storage capacities along the drainage network. An improved means to measure and account for the dynamics of hydrological connectivity at the basin scale is needed to improve prediction of basin scale streamflow. The overall goal of this thesis is to improve the understanding of hydrological connectivity at the basin scale by measuring hydrological connectivity at the Baker Creek Research Basin during 2009. To this end, the objectives are to 1) investigate the dynamics of hydrological connectivity during a typical water year, 2) define the relationship between the contributing stream network and contributing area, 3) investigate how hydrological connectivity influences streamflow, and 4) define how hydrological connectivity influences runoff response to rainfall events. At a 150 km<sup>2</sup> subarctic Precambrian Shield catchment where the poorly-drained heterogeneous mosaic of lakes, exposed bedrock, and soil filled areas creates variable contributing areas, hydrological connectivity was measured between April and September 2009 in 10 sub-basins with a particular focus on three representative sub-basins. The three sub-basins, although of similar relative size, vary considerably in the dominant typology and topology of their constituent elements. At a 10 m spatial resolution, saturated areas were mapped using both multispectral satellite imagery and *in situ* measurements of storage according to land cover. To measure basin scale hydrological connectivity, the drainage network was treated as a graph network with stream reaches being the

edges that connect sub-catchment nodes. The overall hydrological connectivity of the stream network was described as the ratio of actively flowing relative to potentially flowing stream reaches, and the hydrological connectivity of the stream network to the outlet was described as the ratio of actively flowing stream reaches that were connected to the outlet relative to the potentially flowing stream reaches. Hydrological connectivity was highest during the spring freshet but the stream network began to disintegrate with its passing. In some drainage basins, large gate keepers were able to maintain connectivity of the stream network downstream during dry periods. The length of the longest stream was found to be proportional to contributing area raised to a power of 0.605, similar to that noted in Hack's Law and modified Hack's Law relationships. The length of the contributing stream network was also found to be proportional to contributing area raised to a power of 0.851. In general, higher daily average streamflows were noted for higher states of connectivity to the outlet although preliminary investigations allude to the existence of hysteresis in these relationships. Elevated levels of hydrological connectivity were also found to yield higher basin runoff ratios but the shape of the characteristic curve for each basin was heavily influenced by key traits of its land cover heterogeneity. The implications of these findings are that accurate prediction of streamflow and runoff response in a heterogeneous drainage basin with dynamic connectivity will require both an account of the presence or absence of connections but also a differentiation of connection type and an incorporation of aspects of local function that control the flow through connections themselves. The improved understanding of causal factors for the variable streamflow response to runoff generation in this environment will serve as a first step towards developing improved streamflow prediction methods in formerly glaciated landscapes, especially in small ungauged basins.

# TABLE OF CONTENTS

<b>PERMISSION TO USE .....</b>	<b>i</b>
<b>ACKNOWLEDGEMENTS .....</b>	<b>ii</b>
<b>ABSTRACT .....</b>	<b>iv</b>
<b>TABLE OF CONTENTS .....</b>	<b>vi</b>
<b>LIST OF TABLES.....</b>	<b>viii</b>
<b>LIST OF FIGURES.....</b>	<b>ix</b>
<b>LIST OF SYMBOLS .....</b>	<b>xi</b>
<b>CHAPTER 1: INTRODUCTION.....</b>	<b>1</b>
<b>CHAPTER 2: LITERATURE REVIEW .....</b>	<b>3</b>
2.1 CONNECTIVITY .....	3
2.2 HYDROLOGICAL CONNECTIVITY .....	3
2.4 CONNECTIVITY AND MODEL STRUCTURE .....	7
2.5 MEASURING HYDROLOGICAL CONNECTIVITY AT THE BASIN SCALE .....	8
2.6 SUMMARY AND RESEARCH QUESTIONS .....	9
<b>CHAPTER 3: STUDY SITE.....</b>	<b>11</b>
<b>CHAPTER 4: METHODS .....</b>	<b>15</b>
4.1 GROSS DRAINAGE AREA AND DRAINAGE NETWORK .....	15
4.2 ACTIVE AND CONTRIBUTING AREA.....	16
4.3 THE ACTIVE AND CONTRIBUTING STREAM NETWORK.....	20
4.4 QUANTIFYING CONNECTIVITY.....	22
4.5 STREAMFLOW AND RUNOFF RESPONSE .....	23

<b>CHAPTER 5: RESULTS .....</b>	<b>25</b>
5.1 STREAMFLOW .....	25
5.2 DYNAMICS OF ACTIVE AND CONTRIBUTING AREA AND THE STREAM NETWORK .....	26
5.3 CONTRIBUTING STREAM NETWORK AND CONTRIBUTING AREA .....	36
5.4 CONNECTIVITY AND STREAMFLOW .....	37
5.5 CONNECTIVITY AND RUNOFF RESPONSE.....	38
<b>CHAPTER 6: DISCUSSION .....</b>	<b>41</b>
6.1 CONNECTIVITY DYNAMICS.....	41
6.2 CONTRIBUTING STREAM LENGTH AND CONTRIBUTING AREA .....	43
6.3 CONNECTIVITY AND STREAMFLOW .....	45
6.4 CONNECTIVITY AND RUNOFF RESPONSE.....	47
6.5 BASIN CLASSIFICATION BASED ON THE INFLUENCE OF CONNECTIVITY ON RUNOFF RESPONSE .....	49
6.6 DISCUSSION OF LIMITATIONS AND RECOMMENDATIONS .....	51
<b>CHAPTER 6: CONCLUSIONS .....</b>	<b>53</b>
<b>REFERENCES: .....</b>	<b>55</b>
<b>APPENDIX A: RATING CURVES .....</b>	<b>60</b>



## LIST OF TABLES

Table 3.1: Physical characteristics of study basins. For reference, values are included for Baker Creek as a whole. ....	13
Table 5.1: Observed active area, $A_a$ , contributing area, $A_c$ , overall connectivity of the stream network $C_{E,N}$ , and the connectivity of the stream network to the outlet, $C_{E,O}$ . ....	28
Table 5.2: Runoff characteristics observed for rainfall or melt events following satellite image acquisition during 2009.....	39
Table 6.1: Basin classification according to the influence of connectivity on runoff response.....	50

## LIST OF FIGURES

Figure 3.1: Baker Creek Research Basin land cover (SPOT MS satellite imagery May 24, 2008 and June 20, 2009 Composite) and instrument locations. The three study basins Baker Creek below Duckfish Lake, Eagle Pass Creek, and Trail Creek are labeled. Also labeled are lakes mentioned in the text: Duckfish, Great Slave, Landing, Lower Martin, Snowf, Trail, and Vital. The sub-basins used in the analysis of the relationship between contributing stream length and contributing area lie upstream of the streamflow gauges.....14

Figure 5.1: The 2009 streamflow hydrographs for Trail Creek, Eagle Pass Creek, and Baker Creek below Duckfish Lake sub-basins as well as rainfall (P) and snowmelt (M) inputs during 2009. P and M presented in this plot were measured near Vital Lake. Although rainfall is variable throughout the basin, the plot presented here serves as a valid approximation of the magnitude and timing of inputs to the three study basins.....26

Figure 5.2: Storage capacity,  $S_c$ , for terrestrial land covers as well as rainfall, P, and snowmelt, M, inputs during 2009. P and M presented in this plot are for the Baker Creek Research Basin as a whole. Although rainfall is variable throughout the basin, the plot presented here serves as a valid approximation of the magnitude and timing of inputs to the three study basins. .... 27

Figure 5.3: Trail Creek active area (a), contributing area (b), active stream network (c), and contributing stream network (d) for (from left to right) May 9, May 17, June 20, and August 27, 2009..... 29

Figure 5.4: Eagle Pass Creek active area (a), contributing area (b), active stream network (c), and contributing stream network (d) for (from left to right) May 9, May 17, June 20, and August 27, 2009..... 30

Figure 5.5: Baker Creek below Duckfish Lake active area (a), contributing area (b), active stream network (c), and contributing stream network (d) for (from left to right) May 9, May 17, June 20, and August 27, 2009..... 31

Figure 5.6: Active area,  $A_a$  (top), and contributing area,  $A_c$  (bottom), in the three study basins for the days listed in Table II. In the figure above active area and contributing area are presented as percentages of gross drainage area to facilitate comparison. .... 32

Figure 5.7: Overall stream network connectivity,  $C_{E,N}$  (top), and connectivity of the stream network to the outlet,  $C_{E,O}$  (bottom), in the three study basins for the days listed in Table II. The May 9, 2009 and May 17, 2009 values were very similar for most sub-basins..... 33

Figure 5.8: Plot relating contributing stream length,  $L_{s,c}$ , to contributing area,  $A_c$ , (top) and the length of the longest contributing stream,  $L_{s,o}$ , and contributing area (bottom). In the plot of  $L_{s,c}$  vs.  $A_c$  the values while the hydrograph was in recession are marked by white circles and the values while the hydrograph was rising are marked by black circles. Both figures are plotted on a log vs. log scale. .... 36

Figure 5.9: Daily average streamflow,  $Q$  ( $m^3 \cdot s^{-1}$ ), on the satellite image acquisition date defined in Table 3.2, for different states connectivity to the outlet,  $C_{E,O}$ , in the sub-basins of interest. ... 38

Figure 5.10: Runoff ratios,  $R_r$ , observed for different antecedent states of connectivity of the stream network to the outlet,  $C_{E,O}$  (left), and overall connectivity of the stream network,  $C_{E,N}$  (right). .... 40

Figure A.1: Trail Lake streamflow ( $Q$ ) rating curves for stages  $\geq 0$  (level of debris dam) with  $r^2 = 0.87$  and  $Q = 0.0157 + 0.7192 \cdot \text{Stage}$ . .... 60

Figure A.2: Eagle Pass Creek streamflow ( $Q$ ) rating curves for stages  $\geq 0$  (level of earthen dam) with  $r^2 = 0.96$  and  $Q = 6.3234(\text{Stage})^2 + 0.4178(\text{Stage}) - 0.0024$ . .... 59

Figure A.3: Baker Creek below Duckfish Lake streamflow ( $Q$ ) rating curves for stages  $\geq 0$  (level of bedrock sill) with  $r^2 = 0.96$  and  $Q = 1.2861(\text{Stage})^2 + 0.1076(\text{Stage}) - 0.0003$ . .... 59

## LIST OF SYMBOLS

A	Gross drainage area [ $\text{m}^2$ ]
$A_a$	Active area [ $\text{m}^2$ ]
$A_c$	Contributing area [ $\text{m}^2$ ]
$A_l$	Lake area [ $\text{m}^2$ ]
$C_{E,N}$	Overall connectivity
$C_{E,O}$	Connectivity to the outlet
$E_a$	Active edges in the stream network
$E_c$	Contributing edges in the stream network
$E_l$	Lake evaporation [ $\text{mm}\cdot\text{day}^{-1}$ ]
$E_p$	Potential edges in the stream network
$ET_b$	Bedrock evapotranspiration [ $\text{mm}\cdot\text{day}^{-1}$ ]
$ET_t$	Evapotranspiration during transmission [ $\text{m}^3$ ]
h	Hack's law exponent
i	Hydraulic gradient [ $\text{m}\cdot\text{m}^{-1}$ ]
$I_b$	Infiltration to bedrock [ $\text{mm}\cdot\text{day}^{-1}$ ]
L	Length of the longest stream [m]
$L_{s,c}$	Length of contributing streams [m]
$L_{s,o}$	Length of longest contributing stream [m]
LiDAR	Light Detection and Ranging
m.a.l.d.	Meters above local datum [m]
m.a.s.l.	Meters above sea level
M	Melt [mm]
$M_b$	Bedrock melt [ $\text{mm}\cdot\text{day}^{-1}$ ]
$M_e$	Event snowmelt [ $\text{m}^3$ ]
MESH	Modelisation Environnementale Communautaire – Surface Hydrology
MNDWI	Modified normalised difference vegetation index [s.r.u.]
NDVI	Normalised difference vegetation index [s.r.u.]
NIR	Near infrared reflectance [s.r.u.]
$\Delta\text{NIR}$	Change in scaled near infrared reflectance [s.r.u.]
$\Delta\text{NIR}_{\text{image}}$	NIR reflectance change in image [s.r.u.]
$\Delta\text{NIR}_{\text{Phenology}}$	NIR reflectance change due to vegetation phenology change [s.r.u.]
$\Delta\text{NIR}_T$	Threshold change in NIR [s.r.u.]
$\Delta\text{NIR}_{\text{Water}}$	Near infrared reflectance change due to surface water change [s.r.u.]
Q	Daily average streamflow [ $\text{m}^3\cdot\text{s}^{-1}$ ]
$Q_b$	Runoff from bedrock [ $\text{mm}\cdot\text{day}^{-1}$ ]
$q_e$	Average streamflow on the last day of the runoff event [ $\text{m}^3\cdot\text{s}^{-1}$ ]

$Q_e$	Event runoff [ $m^3$ ]
$Q_{in}$	Lake inflow [ $m^3 \cdot s^{-1}$ ]
$q_L$	Infiltration loss [ $m^3$ ]
$q_o$	Antecedent daily average streamflow [ $m^3 \cdot s^{-1}$ ]
$Q_o$	Lake outflow [ $m^3 \cdot s^{-1}$ ]
$P$	Precipitation [mm]
$P_e$	Event precipitation [ $m^3$ ]
$R_r$	Runoff ratio [ $m^3 \cdot m^{-3}$ ]
$\Delta S$	Change in storage [ $mm \cdot day^{-1}$ ]
$\Delta S_b$	Change in bedrock storage [ $mm \cdot day^{-1}$ ]
$S_c$	Storage capacity [mm]
$S_{c,b}$	Bedrock storage capacity [mm]
$S_{c,l}$	Lake storage capacity [m.a.l.d.]
$S_{c,s}$	Soil storage capacity [mm]
$S_{det}$	Detention storage [mm]
$S_{det,l}$	Lake detention storage [m.a.l.d.]
$\Delta S_{det,l}$	Daily change in lake storage [ $m \cdot day^{-1}$ ]
S.R.U	Scaled reflectance units [s.r.u]
$S_s$	Soil storage [mm]
$\Delta S_s$	Change in soil storage [mm]
$\Delta S_{s,s}$	Change in saturated soil storage [mm]
$\Delta S_{s,u}$	Change in unsaturated soil storage [mm]
$S_T$	Threshold storage [mm]
$S_y$	Specific yield
$t^*$	Recession coefficient
$t$	Time [days]
$t_o$	Time of start of rainfall [days]
$t_{qe}$	Time of end of runoff event [days]
$t_{qo}$	Time of start of runoff event [days]
$z$	Depth of soil surface [mm]
$z_T$	Threshold elevation [m.a.l.d]
$z_w(t)$	Water table depth at a time $t$ [mm]
$z_{w,s}$	Water surface elevation [m.a.l.d.]
$\theta$	Volumetric water content [ $m^3 \cdot m^{-3}$ ]

## **CHAPTER 1: INTRODUCTION**

Throughout nature, responses from heterogeneous systems are typically characterized by one or more critical internal thresholds that govern the behaviour of the whole (Sahimi, 1994; Stauffer and Ahorony, 1994; Urban and Keitt, 2001). The presence of these thresholds creates non-linear and hysteretic connectivity among the heterogeneous components within the system. In hydrology, storage thresholds at multiple spatial scales have been repeatedly identified as an important factor in determining the nature of hydrological connectivity (see Spence, 2010 for a review) and hydrological connectivity has been noted to be important in many and various environments (Bracken and Croke, 2007). Despite its noted importance, hydrological connectivity is poorly defined in hydrology (Ali and Roy, 2009) and quantitative investigations are few at the basin scale. In the past, studies of hydrological connectivity have been conducted at small scales. Although research has begun at the basin scale (Jensco et al., 2009) and certain aspects of hydrological connectivity have been incorporated into models (Pomeroy et al., 2007; Reaney et al., 2007; Fang et al., 2010), an explicit quantitative measure of hydrological connectivity at the basin scale is absent from the literature. One is required to improve understanding of non-linear runoff response, further advance model structure, and improve streamflow prediction to better support water management decisions.

The goal of this thesis is to measure hydrological connectivity at the basin scale in order to improve understanding of basin scale hydrological connectivity and its influence on basin streamflow generation. The following chapter will review the literature pertaining to

hydrological connectivity at the basin scale and present the research questions. The study site is described in Chapter 3. The methods used in the study are described in Chapter 4. Chapter 5 will present the results and in Chapter 6 these results will be synthesized and the findings discussed. The conclusions derived from this project are presented in Chapter 7.

## **CHAPTER 2: LITERATURE REVIEW**

### **2.1 Connectivity**

The connectivity of a system is a mature analytical concept in some fields, notably landscape ecology (Kindlmann and Burel, 2008; Goodwin, 2003). In a review of past quantitative investigations addressing ecological connectivity, Kindlmann and Burel (2008) simply define connectivity in a landscape ecology context as a “measure of easiness of movement.” Metrics created in landscape ecology for the quantitative analysis of spatial connectivity have been defined either structurally, as an attribute of only landscape structure, or functionally, incorporating aspects of landscape structure as well as species response to landscape structure (Goodwin 2003). Goodwin (2003) note that the majority of studies basing metrics of connectivity on the structural characteristics of the landscape treat it as an independent variable while studies that base connectivity on the movement of organisms treat connectivity as dependent on both landscape structure and ecological processes.

### **2.2 Hydrological connectivity**

In hydrology, the definition and practical application of the term “hydrological connectivity” has been ambiguous and varied. In a review of “hydrological connectivity,” Ali and Roy (2009) found that it has been used to define 1) attributes of the water cycle and its components, 2) geomorphological or landscape features, 3) hydrological properties, or 4) flow processes. Hydrologists should be interested in connectivity in its functional sense so that connectivity



should be considered as a measure of whether or not the constituent parts of the basin can transfer water through the drainage network. Bracken and Croke (2007) aptly defined hydrological connectivity as the ability to transfer water from one part of a landscape to another. A measurement of basin scale hydrological connectivity should provide a quantitative expression of the degree to which water can move throughout the drainage basin.

Hydrological connectivity is crucial for understanding runoff response at the larger basin scale because 1) the topographic bounds of a basin constitute the gross drainage area but not necessarily the contributing area, and 2) the stream network is rarely synonymous with the drainage network. As a result, active areas which are saturated and can generate runoff, are not necessarily contributing areas which are active and hydrologically connected to the outlet (Ambroise, 2004). All points within the gross drainage area could contribute runoff to the outlet of the catchment if they were saturated and connected to the outlet by other saturated areas or flow pathways. Non-contributing active areas generate runoff which is transferred downstream but does not reach the outlet. In its fully connected or maximum state, the stream network is synonymous with the drainage network, has one component and runoff from the entire gross drainage area may be transmitted through the stream network to the basin outlet. When storage deficits occur within the drainage basin and along the drainage network, the stream network is segmented into one component connected to the outlet and one or more internally drained components not connected to the outlet.

In keeping with the loose definition provided by Bracken and Croke (2007), the review by Ali and Roy (2009) and precedents from landscape ecology (Kindlmann and Burel, 2008; Urban and

Keitt, 2001), the hydrological connectivity of a drainage network can be conceptualized as a dependent state variable controlled by several factors that are both static and dynamic. The static factors influencing connectivity are implicitly linked to overall catchment pattern which is governed by its composition of structural elements and the manner in which they are configured (Schröder, 2006; Jensco et al., 2009). Therefore, the primary static controls are those Buttle (2004) proposed as the primary controls on streamflow generation. The typology of hydrological elements influences the relative predominance of hydrological processes (Buttle, 2004; Allan and Roulet, 1994), threshold storage capacities, and residence times. The topology of elements influences the intensity and duration of upstream contributions (Mielko and Woo, 2006) and thus the probability of connection and relative role in runoff response (Woo and Mielko, 2007; Spence, 2007). The topography dictates the gradients and path of the network of potential hydrological connections. Slope and micro-topography are also important in determining depressional storage capacities (Spence and Woo, 2002; Kirkby et al. 2002). The key dynamic factors influencing connectivity are the relative rates of hydrological processes (Spence, 2006; Woo and Mielko, 2007) and variation in the energy required to drive these processes (Pomeroy et al., 2003; Quinton and Carey 2008). In an area of discontinuous permafrost, below ground storage capacity of soil filled areas is also dynamic: It is least at the end of winter and increases as the frost depth retreats with the melting of the frozen soils (Gray et al. 2001; Quinton and Marsh, 1999).

The concept of hydrological connectivity, through its association with variable contributing area, has been noted in different forms for some time in prairie environments (Stichling and Blackwell, 1957) and the Precambrian shield (Park, 1979). Given that there is variable

contributing area in these environments, it would follow that the associated stream network would vary as well. In the recurring relationship between absolute stream length and drainage area defined by Hack's Law (Hack 1957) and modifications of it (Gray, 1961; Muller, 1979; Rigon, 1996), the absolute length of a stream is functionally related to the area upstream (Rodriguez-Iturbe and Rinaldo, 1997). Traditionally, Hack's Law relationships have been used to relate gross drainage area and the longest stream in the drainage network. However as previously stated, contributing area and contributing stream length are rarely synonymous with the gross drainage area and the drainage network. As a result, in many Canadian landscapes variable contributing area and variable stream network connectivity usually render the absolute length of a stream irrelevant. Regardless, the length of the longest stream is often used as a parameter related to the time of concentration during runoff response and stream length in general is often used as a parameter in streamflow routing routines. Relationships linking contributing area and contributing stream length are missing from the literature and are necessary to support the incorporation of dynamic contributing area and contributing stream length into simple streamflow and runoff response modelling applications.

Hydrological connectivity has been shown to be important to non-linear runoff response at the hillslope scale in a wide variety of landscapes including the boreal plains (Quinton et al. 2003), Precambrian Shield (Spence and Woo, 2002; Buttle et al., 2004; James and Roulet, 2007; Mielko and Woo, 2006), prairie and rangelands (Western et al., 2001; Shaw et al., 2009; Fang et al., 2010), and temperate forests (Tromp van Meerveld and McDonnell, 2006; Lehmann et al., 2007). Jenco et al. (2009) also demonstrated the importance of connectivity between hillslope, riparian, and stream water tables in a high relief environment where the fraction of the stream

network connected to its uplands controlled runoff magnitude at the basin scale. Recent studies of hydrological connectivity have often been conducted at a small scale and have focused on the spatial connectivity of hydrological properties (Western et al., 2001; James and Roulet, 2004; Lehman et al., 2007). Research at the basin scale has begun quantifying connectivity according to the magnitude and duration of the connectivity of upstream areas (Jensco et al., 2009). However, hydrological connectivity has not been explicitly measured and accounted for at the basin scale and an improved means to measure and account for the dynamics of stream network connectivity is necessary to improve the prediction of streamflow at the basin scale, especially in ungauged basins.

#### **2.4 Connectivity and Model Structure**

Some aspects of the concept of hydrological connectivity have been incorporated into physically based hydrological models. In the Connectivity of Runoff Model, CRUM (Reaney et al., 2007), designed for the analysis of distributed runoff generation from a hillslope with variable rainfall inputs, connectivity is incorporated by partitioning runoff generation processes into 1) all water infiltrating, 2) the surface depression store filling or emptying without runoff occurring, 3) the generation and transmission of runoff, and 4) the transmission of runoff without new runoff being generated. In this way, the variability in spatial connectivity of runoff generation and transmission is accounted for by the necessity of filling stores at the hillslope scale before runoff can be generated. In the Cold Regions Hydrological Model, CRHM, a physically based modelling platform, aspects of runoff connectivity are accounted for using a cascading sequence of hydrological response units, HRU (Pomeroy et al., 2007). If depression storage is not full, an HRU cannot transmit flow and does not connect upstream HRU's. If an HRU's depression

storage is full, runoff generated in the upstream HRU is transmitted downstream. Other commonly used Canadian hydrological models such as WATFLOOD (Kouwen, 2010) and MESH (Pietroniro et al., 2007) do not presently incorporate connectivity in their model structure.

## **2.5 Measuring hydrological connectivity at the basin scale**

In this thesis, a means to measure basin scale connectivity is introduced that uses aspects of graph theory (Chartrand, 1977; Gross and Yellen, 2006) to describe the drainage network and active stream network from which connectivity is measured while accommodating the heterogeneity of the landscape. Measuring the active stream network is made possible by mapping storage states throughout the drainage basin. Mapping storage states at the basin scale in a heterogeneous landscape requires the integration of data from several sources. In a study of storage dynamics and contributing area, Spence et al. (2010) used point measurements in sites representative of land cover units which repeat themselves over large scales. Storage state at the basin scale was mapped by extrapolating measurements from the representative sites by land cover type. Lumping storage state by land cover serves as a valid approximation of storage at large scales during wet periods but underestimates inundated areas where water concentrates during dry periods. The remote sensing of surface ponding has also been used to monitor connectivity of very wet landscapes (Töyrä and Pietrienero, 2003). Remote sensing is useful mostly for the detection and mapping of inundated areas and its ability to do so is limited by its spatial resolution. During wet periods, the use of remote sensing may underestimate the extent of saturated areas that are not inundated with water. A composite of the two methods may provide a more robust approach to mapping saturated terrestrial areas during both wet and dry periods. In wet periods, it will provide a more accurate depiction of the extent of saturated areas

and in dry periods, it will still detect inundated areas that differ from the general land cover response.

## **2.6 Summary and research questions**

Connectivity is a mature analytical concept in other fields, most notably landscape ecology where it is taken to be a measure of the easiness of movement within a system. Hydrological connectivity is poorly defined but should be considered as a measure of the degree to which water can move throughout the basin. The variability of hydrological connectivity is influenced by landscape structure and hydrological processes. Variation in hydrological connectivity is important because it influences drainage basin runoff response. This importance has been acknowledged for some time and in various landscapes. Although hydrological connectivity has been measured at small scales and some aspects of connectivity have been incorporated into models, quantitative analysis of basin scale hydrological connectivity is absent in the literature. A representation of a drainage basin as a graph network will facilitate the measurement of hydrological connectivity at the basin scale while accommodating important traits of land cover heterogeneity. Storage state will be measured using a composite of on-site measurements and remote sensing products. Measures of hydrological connectivity will be derived from the active and contributing stream network. In this thesis, these measures will be applied to the Baker Creek Research Basin, a watershed whose contributing area has been noted to be extremely variable in the past (Park, 1979; Spence , 2006; Gibson and Reid, 2010; Spence et al., 2010) and where connectivity is expected to be important. The goal of this thesis is to improve understanding of hydrological connectivity at the basin scale and establish what influence it has

on streamflow generation. To achieve this goal, the following research questions will be addressed:

1. What are the dynamics of hydrological connectivity throughout a typical water year?
2. What is the relationship between the contributing stream network and contributing area?
3. How does hydrological connectivity influence streamflow?
4. How does hydrological connectivity influence s runoff response to rainfall events?

### **CHAPTER 3: STUDY SITE**

The Baker Creek Research basin (center at 62°35'N, 114°26'W) and nine of its sub-basins located upstream of stream flow gauge sites (Figure 3.1) were used in this study conducted between April 10, 2009 and September 30, 2009. Three distinctive sub-catchments within the Baker Creek Research Basin were selected for the detailed study of connectivity dynamics and their influence on streamflow generation (Figure 3.1; Table 3.1). Baker Creek below Duckfish Lake, Eagle Pass Creek (not official name), and Trail Creek (not official name) each drain 25, 21, and 8 km<sup>2</sup>, respectively. These catchments are located in the Great Slave Upland High Boreal Ecoregion (Ecosystem Classification Group, 2008) and the Slave structural province of the Precambrian Shield (Kerr and Wilson, 2003). Total relief in each watershed is low and varies from 16 – 35 m (Table 3.1). The terrestrial landscape can be divided into five common land covers: coniferous forest, deciduous forest, open peatlands, wetlands, and exposed bedrock (Figure 3.1). The percentage cover of each land cover differs for each basin (Table 3.1). Forest soil profiles are typically a thin organic layer overlying mineral soil (Ecosystem Classification Group, 2008). Open peatlands situated in depressions in the rolling bedrock cover 6%, 11% and 9% of the Trail, Eagle Pass and Baker Creek below Duckfish basins, respectively. They consist of a layer of peat averaging 1.2m deep overlying bedrock. Wetlands have an organic layer (Ecosystem Classification Group, 2008), averaging 0.4m in depth, overlying glaciolacustrine deposits. The bedrock surface is moderately to highly fractured with silty sandy soils from the weathering and erosion of bedrock filling some cracks. Permafrost is discontinuous and absent from exposed bedrock, well drained areas and areas adjacent to water courses (Wolfe, 1998). There are on average 30 lakes in each of the study basins that cover approximately 6%, 16% and



23% of the Trail Creek, Eagle Pass Creek and Baker Creek below Duckfish Lake basins, respectively. The Trail Creek drainage network contains the smallest lakes, on average, in the three basins. Eagle Pass Creek is a chain of lakes connected by short channels. The drainage network of Baker Creek below Duckfish Lake is dominated by the 6 km<sup>2</sup> Duckfish Lake immediately upstream of the gauging site. The four study basins described in Table 3.1 as well as six other sub-basins located upstream of streamflow gauges in the Baker Creek Research Basin (Figure 3.1) were used in the analysis of the relationship between contributing stream length and contributing area as well as the relationship between the longest contributing stream and contributing area.

Table 3.1: Physical characteristics of study basins. For reference, values are included for Baker Creek as a whole.

Drainage Basin	Area (km <sup>2</sup> )	Relief (m)	Coniferous forest	Lake	Deciduous forest	Open peatland	Wetland	Exposed bedrock	Number of lakes	Mean lake area (m <sup>2</sup> )
Trail Creek	8	46	4%	6%	0%	6%	3%	82%	27	39,786
Eagle Pass Creek	21	28	25%	16%	1%	11%	5%	43%	31	120,577
B.C. below Duckfish Lake	25	35	14%	23%	0%	9%	2%	52%	31	279,306
B.C. below Lower Martin Lake	153	65	21%	23%	1%	10%	6%	40%	349	88,800

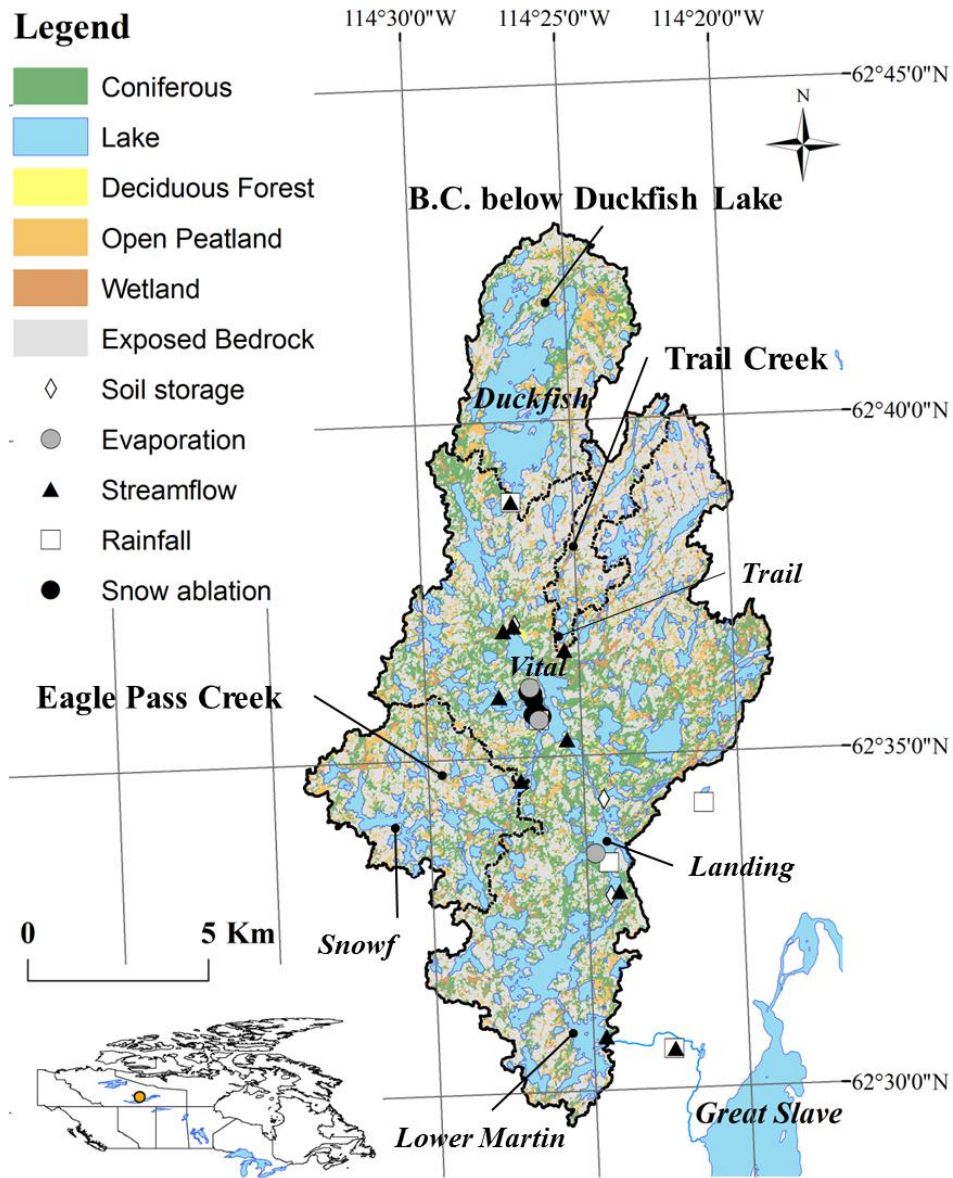


Figure 3.1: Baker Creek Research Basin land cover (SPOT MS satellite imagery May 24, 2008 and June 20, 2009 Composite) and instrument locations. The three study basins Baker Creek below Duckfish Lake, Eagle Pass Creek, and Trail Creek are labeled. Also labeled are lakes mentioned in the text: Duckfish, Great Slave, Landing, Lower Martin, Snowf, Trail, and Vital. The sub-basins used in the analysis of the relationship between contributing stream length and contributing area lie upstream of the streamflow gauges.

## **CHAPTER 4: METHODS**

### **4.1 Gross drainage area and drainage network**

The gross drainage area, five hectare sub-catchments and drainage network were derived from a 1m LiDAR digital elevation model (DEM) re-sampled to a 10m spatial resolution for computational efficiency. A graph network, a description of a system as nodes and edges, was built from the land cover and drainage network (Gross and Yellen, 2006). In a graph network, nodes represent a system's parts and edges represent some relationship between the parts. The nodes were taken to be five hectare headwater terrestrial sub-catchments, five hectare receiving terrestrial sub-catchments, and lakes. The edges were taken to be the streams connecting the nodes. Land cover was mapped using a maximum likelihood supervised classification of a composite image that combined two SPOT5 MS satellite images collected on May 24, 2008 prior to the emergence of leaves and on June 20, 2009 following leaf out. The SPOT5 MS satellite imagery had a 10m spatial resolution. The four multispectral bands and the normalized difference vegetation index, NDVI (McFeeters, 1996), of both images were used as input information. Following classification, a mode based filter with a 3 cell by 3 cell mask was passed over the image to filter out errors commonly experienced at edges due to mixed pixel signatures. The accuracy of the land cover classification was evaluated using a random sample of 314 points recorded during field surveys and marked with a handheld global positioning system (GPS) accurate to within  $\pm 8\text{m}$ . The overall accuracy of the land cover map was 86% and the kappa coefficient (Congalton, 1991) was 0.82.

## 4.2 Active and contributing area

Mapping the active area,  $A_a$  ( $m^2$ ), contributing area,  $A_c$  ( $m^2$ ), and stream network required the mapping of storage states within the sub-catchments. Wells installed to the 2007 maximum depth of thaw at six representative sites (two each in open peatlands, wetlands and forests) were equipped with Solinst submersible pressure transducers to measure water table depth,  $z_{w(t)}$  (mm), half hourly for the period April to September, 2009. Water table depth was measured manually relative to the depth of the ground surface,  $z$  (mm), at least every two weeks at each of the sites to validate pressure transducer readings and when pressure transducers were frozen beneath ice, manual measurements were taken every two days. Adjacent to each well, volumetric soil moisture content,  $\theta$  ( $m^3 \cdot m^{-3}$ ), was measured half hourly with a string of two site specific calibrated Decagon Devices ECH<sub>2</sub>O TE probes installed horizontally at the soil surface and at a depth of 250 mm below the ground surface. For a soil filled land cover, the change in storage upon the day previous,  $\Delta S$  (mm), was calculated as the sum of the change in unsaturated soil storage,  $\Delta S_{s,u}$  (mm), and change in saturated soil storage,  $\Delta S_{s,s}$  (mm). Values of specific yield,  $S_y$ , were those used by Spence et al. (2010).

$$\Delta S = \Delta S_u + \Delta S_s \quad (1)$$

$$\Delta S = \Delta \theta [z - z_{w(t)}] + S_y [z_{w(t)} - z_{w(t-1)}] \quad (2)$$

Soil storage was calculated as the sum of the soil storage in the previous day,  $S_s$  (mm), and  $\Delta S$ .

$$S_{si(t)} = S_{si(t-1)} + \Delta S \quad (3)$$

The soil storage capacity ( $S_{c,s}$ ) was calculated by subtracting  $S_s$  from the threshold storage capacity  $S_t$ . The  $S_{ci}$  was zero when the water table was equal to or greater than the elevation of the ground surface.

$$S_{ci(t)} = S_t - S_{si(t)} \quad (4)$$

A soil filled land cover type was considered active when the water table was equal to or greater than the elevation of the ground surface or the soil was saturated and the  $S_c$  was equal to 0.

The water budget of exposed bedrock was calculated with a model in which all terms are in units of  $\text{mm}\cdot\text{d}^{-1}$ :

$$\Delta S_b = P + M_b - ET_b - I_b - Q_b \quad (5)$$

Rainfall,  $P$ , was measured with a continuously recording Texas Electronics TR-525M tipping bucket rain gauge and accumulations were confirmed with an Meteorological Service of Canada Type B storage rain gauge. Snowmelt,  $M_b$ , was measured at a bedrock outcrop close to Vital Lake daily using an ablation line and snow survey methods similar to Heron and Woo (1978). Evapotranspiration over bedrock,  $ET_b$ , was measured directly with an eddy covariance system consisting of a three dimensional sonic anemometer and an open path gas analyzer. Measurements of wind speed and water vapour content were taken at 10 Hz and fluxes calculated over a half hour period. Corrections to the eddy covariance measurements included coordinate rotation (Kaimal and Finnigan, 1994), the WPL adjustment (Webb et al., 1980), and those for sonic path length, high frequency attenuation, sensor separation (Massman, 2000; Horst, 1997) and oxygen extinction. Infiltration to bedrock,  $I_b$ , was estimated to be  $1.07 \text{ mm}\cdot\text{day}^{-1}$ , calculated using a parallel plate model as in Domenico and Schwartz (1998) for eight  $3 \text{ m} \times 3 \text{ m}$  plots of exposed bedrock at Baker Creek. The model assumed that  $P$  and  $M_b$  inputs would first infiltrate, with any excess water evaporating at the rate defined by  $ET_b$ . Remaining water was stored until storage capacity was filled and then the remainder would run off,  $Q_b$ . On a bedrock slope adjacent to Camp Wetland, three weirs with contributing areas of  $64 \text{ m}^2$ ,  $38 \text{ m}^2$ , and  $11 \text{ m}^2$  were installed to observe bedrock runoff and validate the water budget model. When

initially at maximum storage capacity, the contributing area of the weirs required an application of 7.8 mm precipitation before running off. Accordingly, the absolute storage capacity for bedrock was taken to be 7.8 mm. Once dry, the bedrock returned to its absolute storage capacity. The daily storage capacity for a unit area of exposed bedrock,  $S_{c,b}$  (mm), was calculated as the change in storage capacity,  $\Delta S_b$  (mm), from the previous day.

$$S_{c,b(t)} = S_{c,b(t-1)} + \Delta S_{b(t)} \quad (6)$$

When  $S_{c,b}$  was 0, the bedrock was considered active. The bedrock model always accurately simulated days when each plot became saturated and produced runoff. These field observations were extrapolated over space using the distribution of bedrock in the SPOT land cover map.

To supplement the field observations of terrestrial storage, surface ponding was mapped on May 17, June 20, and August 27, 2009 using SPOT5 MS satellite imagery. Prior to processing, all images were atmospherically corrected and each image was orthorectified with at least 15 ground control points producing a root mean square error of less than  $\pm 0.2$  pixels. A supervised maximum likelihood classifier was used to classify saturated terrestrial, unsaturated terrestrial, snow/ice and open water areas in the base image collected on May 17, 2009. The four multispectral bands and the modified normalized difference water index, MNDWI (Xu, 2006), were used as input information. Training areas were selected based on notes and photographs taken during field work around the acquisition date. Two hundred and fourteen ground control points around Vital Lake were visited on May 23-25, 2009 for ground truthing and accuracy assessment of the classification. The accuracy assessment of the classification yielded an overall accuracy of 85% and a kappa coefficient (Congalton, 1991) of 0.75.

Surface ponding was mapped for June 20, 2009 and August 27, 2009 based on change relative to the initial ponding classification. A simple differencing approach based on change in scaled NIR reflectance,  $\Delta\text{NIR}$  (scaled reflectance units), was used to create a binary change mask. This was used to distinguish amongst ice, water, and non-water covered surfaces. Values of  $\Delta\text{NIR}$  were compared to a threshold  $\Delta\text{NIR}_T$ , change between the base image and the change image.  $\Delta\text{NIR}$  was taken to be the sum of a base change associated with each image,  $\Delta\text{NIR}_{\text{image}}$ , NIR change due to changes in vegetation phenology,  $\Delta\text{NIR}_{\text{Phenology}}$ , and NIR change due to the disappearance of surface ponding in the change image where it had been in the base image,  $\Delta\text{NIR}_{\text{Water}}$ .  $\Delta\text{NIR}_{\text{Image}}$  is consistent throughout the scene and  $\Delta\text{NIR}_{\text{Phenology}}$  is consistent for areas of similar land cover type. NIR changes in excess of changes due to  $\Delta\text{NIR}_{\text{Phenology}}$  and  $\Delta\text{NIR}_{\text{Image}}$  are expected to result from  $\Delta\text{NIR}_{\text{Water}}$ .

$$\Delta\text{NIR} = \text{NIR}_{\text{Date2}} - \text{NIR}_{\text{BaseImage}} \quad (7)$$

$$\Delta\text{NIR} = \Delta\text{NIR}_{\text{Water}} + \Delta\text{NIR}_{\text{Phenology}} + \Delta\text{NIR}_{\text{Image}} \quad (8)$$

$$\Delta\text{NIR}_{\text{Water}} = \Delta\text{NIR} - \Delta\text{NIR}_{\text{Phenology}} - \Delta\text{NIR}_{\text{Image}} \quad (9)$$

$\Delta\text{NIR}$  values were extracted from training areas for each land cover. A K-means cluster analysis was used to identify the centers of two distinct clusters and identify  $\Delta\text{NIR}_T$ , the boundary separating the upper and lower cluster. The values belonging to the lower cluster express  $\Delta\text{NIR}_{\text{Image}}$  and  $\Delta\text{NIR}_{\text{Phenology}}$ . The values belonging to the upper cluster were presumed to express  $\Delta\text{NIR}_{\text{Image}}$ ,  $\Delta\text{NIR}_{\text{Phenology}}$ , and  $\Delta\text{NIR}_{\text{Water}}$ . Cells with a value in the lower cluster were deemed to have not changed wetness state from the base image, and vice versa. In the instance where ice was present on May 17, 2009, a k-means cluster analysis was conducted to separate  $\Delta\text{NIR}$  into two classes. The cluster having the lowest value was presumed to signal a change



from ice to water. The upper cluster was presumed to signal a change from ice to unsaturated terrestrial.

Lake level,  $z_{w.s.}$ , expressed in units of metres above an arbitrary local datum (m.a.l.d.), was measured half hourly at five lakes of different sizes using submersible Solinst Levellogger Gold Model 3001 pressure transducers referenced to a Solinst Barologger. Water surface elevation was manually tied to local bench marks at least once every two weeks and more often during April and May. Lakes become active when a threshold outlet elevation,  $z_T$  (m.a.l.d.) is exceeded and outflow is generated from detention storage,  $S_{det,l}$  (mm).  $S_{det,l}$  is the height of  $z_{w.s.}$  above  $z_T$  and lakes with  $S_{det,l}$  values greater than or equal to  $z_T$  were considered to be active. The  $z_T$  was defined with manual surveys at each monitored lake. Daily relationships between  $S_{det,l}$  and lake area,  $A_l$  ( $m^2$ ), were defined and used to estimate  $S_{det,l}$  in non-instrumented lakes throughout the basin. This method yields  $S_{det,l}$  values within 15% of observed values at instrumented lakes.

Active area was thus mapped as any areas deemed to be active through the *in situ* measurement of storage by land cover or the remote sensing of surface ponding. Contributing area was defined as the active areas with a contiguous downstream path of active area to the outlet through adjacent or diagonal relationships.

### **4.3 The active and contributing stream network**

Sub-catchments were considered active if runoff was generated within them. For lake sub-catchments, this was indicated by outflow. For terrestrial sub-catchments this was indicated by the presence of active areas. The method by which the active stream network was selected from

the drainage network depended on whether a node was a 1) headwater terrestrial sub-catchment, 2) receiving terrestrial sub-catchment, or 3) lake. A stream out of a terrestrial headwater sub-catchment was identified if there was a contiguous active area path downstream to the next sub-catchment or lake shoreline. Streams were identified through a receiving terrestrial sub-catchment by contiguous active area drainage paths to the next downstream sub-catchment. If a receiving sub-catchment was disconnected from upstream, its function reverted to that of a headwater sub-catchment. A simple lumped flow routing model was used to estimate where stream connections existed downstream of lakes. The emergence of a stream from a lake was taken to exist if the transfer of  $S_{\text{det},l}$  out of the upstream lake was sufficient to overcome vertical and lateral losses while being conveyed downstream. Starting from a headwater location, the connectivity of the headwater lake to the next downstream lake was established through the routing of daily changes in lake detention storage,  $\Delta S_{\text{det},l}$  ( $\text{mm}\cdot\text{day}^{-1}$ ).

$$\Delta S_{\text{det},l_i} = S_{\text{det},l_i(t)} - S_{\text{det},l_i(t-1)} \quad (10)$$

$$Q_{o,l_i} = \Delta S_{\text{det},l_i} - E_{l_i} \quad (11)$$

Lake outflow,  $Q_{o,l}$  ( $\text{mm}\cdot\text{day}^{-1}$ ), was taken to be the  $\Delta S_{\text{det},l}$  remaining after losses to lake evaporation  $E_l$  ( $\text{mm}\cdot\text{day}^{-1}$ ). The latter was estimated from daily measurements from an eddy covariance system on a rock outcrop in Landing Lake (Granger and Hedstrom, 2010).

Lateral and vertical losses during transmission through stream reaches were estimated assuming a trapezoidal channel of uniform width and depth comparable to instrumented streams in the basin (Spence et al., 2010). Evapotranspiration during transmission ( $ET_t$ ) was calculated using methods defined in Guan et al. (2010). Infiltration loss,  $q_L$  ( $\text{m}^3$ ) during transmission was estimated using Darcy's law using hydraulic gradients,  $i$  ( $\text{m}\cdot\text{m}^{-1}$ ), measured near instrumented

streams and hydraulic conductivities from Guan et al. (2010). Flow not consumed by losses during transmission of water between lakes was added to the next lake in the chain.

$$Q_{in,l_{i+1}} = Q_{0,l_i} - ET_T - q_L \quad (12)$$

A connection existed from one lake to the next if inflow to the next lake in the chain,  $Q_{in,l_{i+1}}$  (mm), exceeded losses during transmission and was greater than 0.

#### 4.4 Quantifying connectivity

The overall connectivity of the stream network is a measure in some ways comparable to the wetness state of the basin. The connectivity of the stream network  $C_{E,N}$  was taken to be the ratio of edges in the active stream network,  $E_a$ , to the total number of edges in the drainage network,  $E_p$ .

$$C_{E,N} = \frac{E_a}{E_p} \quad (13)$$

The connectivity to the outlet,  $C_{E,o}$ , however, is a measure of the stream network's ability to transfer antecedent and event water to the outlet. The connectivity of the stream network to the outlet,  $C_{E,O}$ , was defined as the ratio of contributing edges,  $E_c$ , to  $E_p$ .

$$C_{E,O} = \frac{E_c}{E_p} \quad (14)$$

The cumulative length of the contributing edges was summed to find the length of the contributing stream network,  $L_{s,c}$  (m), and the longest contributing stream was isolated and measured to find  $L_{s,o}$  (m). Both lengths were measured for the Baker Creek Research Basin as a whole and nine of its nested sub-basins on May 9, May 17, June 20, and August 27, 2009. The sub-basins lie upstream of the streamflow gauges shown in Figure 3.1.

#### 4.5 Streamflow and runoff response

Streamflow was observed at the outlets of headwater lakes, in tributaries, and in a nested fashion along Baker Creek (Figure 3.1). The flow at Lower Martin Lake outlet was measured at the Water Survey of Canada (WSC) hydrometric gauge 07SB013. At all other sites streamflow was measured periodically using area-velocity methods based on velocity measurements made using a SONTEK FloTracker Acoustic flow meter. Stage-discharge relationships were developed for each site from observed streamflow and corresponding manually surveyed lake levels.

To investigate the influence of connectivity on runoff response, event volume,  $Q_e$  ( $m^3$ ), was estimated by separating storm flow from the hydrograph using an exponential decay function (Dingman, 1973):

$$Q_e = \int_{t_{q_0}}^{t_{q_e}} \left( q - \left( q_0 \cdot e^{\left( \frac{-t}{\tau} \right)} \right) \right) dt \quad (15)$$

Where  $q$  ( $m^3 \cdot s^{-1}$ ), is the observed daily average streamflow,  $q_0$  ( $m^3 \cdot s^{-1}$ ) is the daily average streamflow on the day preceding rainfall,  $q_e$  ( $m^3 \cdot s^{-1}$ ) is the daily average streamflow on the last day of the runoff event, and  $t$  (days) is the time since the beginning of the rain event. The

recession coefficient,  $t^*$ , was calculated as the reciprocal to the slope of a plot of  $\ln(q)$  versus  $t$  for the receding limb of the hydrograph prior to interruption by the rain event (McNamara et al., 1998). The runoff ratio,  $R_r$  was calculated as:

$$R_r = \frac{Q_e}{P_e + M_e} \quad (16)$$

Rainfall,  $P$  (mm), was measured with continuously recording Texas Electronics TR-525M tipping bucket rain gauges at three sites in the Baker Creek Research Basin and at two sites located just outside the basin boundary (Figure 3.1). Meteorological Service of Canada Type B manual rain gauges were used at four of five sampling points to validate tipping bucket measurements. At the four gauge sites equipped with both instruments, the error observed between the cumulative precipitation measured by the tipping bucket and Type B rain gauges was -2%, 5%, 5% and 3% respectively. Sub-basin rainfall was estimated using Thiessen polygons around the five precipitation measurement sites. Melt,  $M$  (mm), was measured using ablation lines and methods similar to Heron and Woo (1978) at one site for each land cover located around Vital Lake (Figure 3.1). Daily melt was calculated for each sub-basin as the product of the daily melt in a land cover, the observed snow covered fraction in that land cover, and the area of the land cover within the sub-basin. Sub-basin inputs for a given runoff event were taken to be sum of rainfall for the event,  $P_e$  ( $m^3$ ), and snowmelt for the event,  $M_e$  ( $m^3$ ).

## CHAPTER 5: RESULTS

### 5.1 Streamflow

The level of Trail Lake rose above its debris dam on April 30 and streamflow in Trail Creek rose sharply to a peak of  $0.124 \text{ m}^3 \cdot \text{s}^{-1}$  on May 4 (Figure 5.1). The Eagle Pass Creek sub-basin began flowing at its outlet on May 4 and peaked at  $0.274 \text{ m}^3 \cdot \text{s}^{-1}$  on May 12 (Figure 5.1). Baker Creek below Duckfish Lake maintained connection throughout the winter of 2008-2009 and was flowing before the spring freshet. Baker Creek below Duckfish Lake peaked at  $0.159 \text{ m}^3 \cdot \text{s}^{-1}$  on May 20. The recession of Trail Creek flow was abrupt and streamflow fell sharply through May and June following the spring freshet (Figure 5.1). The level of Trail Lake declined to the outlet's debris dam elevation on June 18 and flow dropped to  $0.021 \text{ m}^3 \cdot \text{s}^{-1}$ . Following a short-term response to the June 23 and July 1-3 rainfall events, Trail Lake once again fell below its debris dam on July 13 and flow slowed to lower than  $0.016 \text{ m}^3 \cdot \text{s}^{-1}$  for the duration of the study period. Eagle Pass Creek's recession during late May and early June was gradual and interrupted by responses to even small rainfall events (Figures 5.1). The recession of flow in Baker Creek below Duckfish Lake was gradual through May and June but grew steeper in early July as evapotranspiration and infiltration losses increased (Figure 5.1). At the end of September, several small rainfall events occurred in close succession and caused streamflow to rise in the Duckfish Lake and Eagle Pass Creek sub-basins (Figure 5.1). The level of Trail Lake rose but only reached the level of its debris dam on October 1 and as a result, a rise in stream flow was not observed (Figure 5.1).

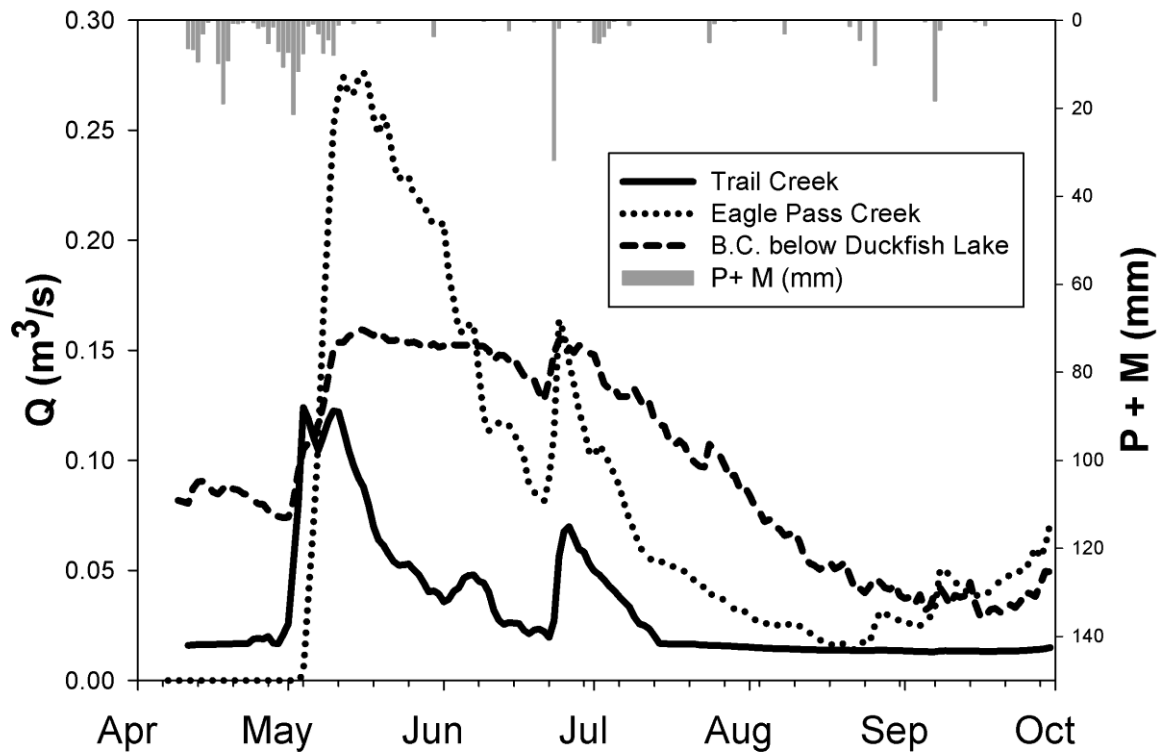


Figure 5.1: The 2009 streamflow hydrographs for Trail Creek, Eagle Pass Creek, and Baker Creek below Duckfish Lake sub-basins as well as rainfall (P) and snowmelt (M) inputs during 2009. P and M presented in this plot were measured near Vital Lake. Although rainfall is variable throughout the basin, the plot presented here serves as a valid approximation of the magnitude and timing of inputs to the three study basins.

### Me 5.2 Dynamics of active and contributing area and the stream network

Much of the lake modulated stream network was disconnected at the beginning of the 2009 water year. The melt period began on April 10 and on May 9 all terrestrial land covers were active (Figure 5.2). Lake storage capacity was overcome and active and contributing areas were the same as the gross drainage area (Figures 5.3, 5.4, 5.5 and 5.6, Table 5.1) while the stream network was synonymous with the drainage network (Figure 5.7). The majority of forest and exposed bedrock areas became inactive on May 11 and 12 respectively (Figure 5.2) causing a

small number of headwater terrestrial sub-catchments to disconnect. By May 17 active area and contributing area had fallen (Figure 5.6 and Table 5.1) as large tracts of forest and exposed bedrock became inactive. However, storage capacity remained satisfied in peatlands (Figure 5.2) and headwater lakes and  $C_{E,O}$  and  $C_{E,N}$  remained high (Figure 5.7).

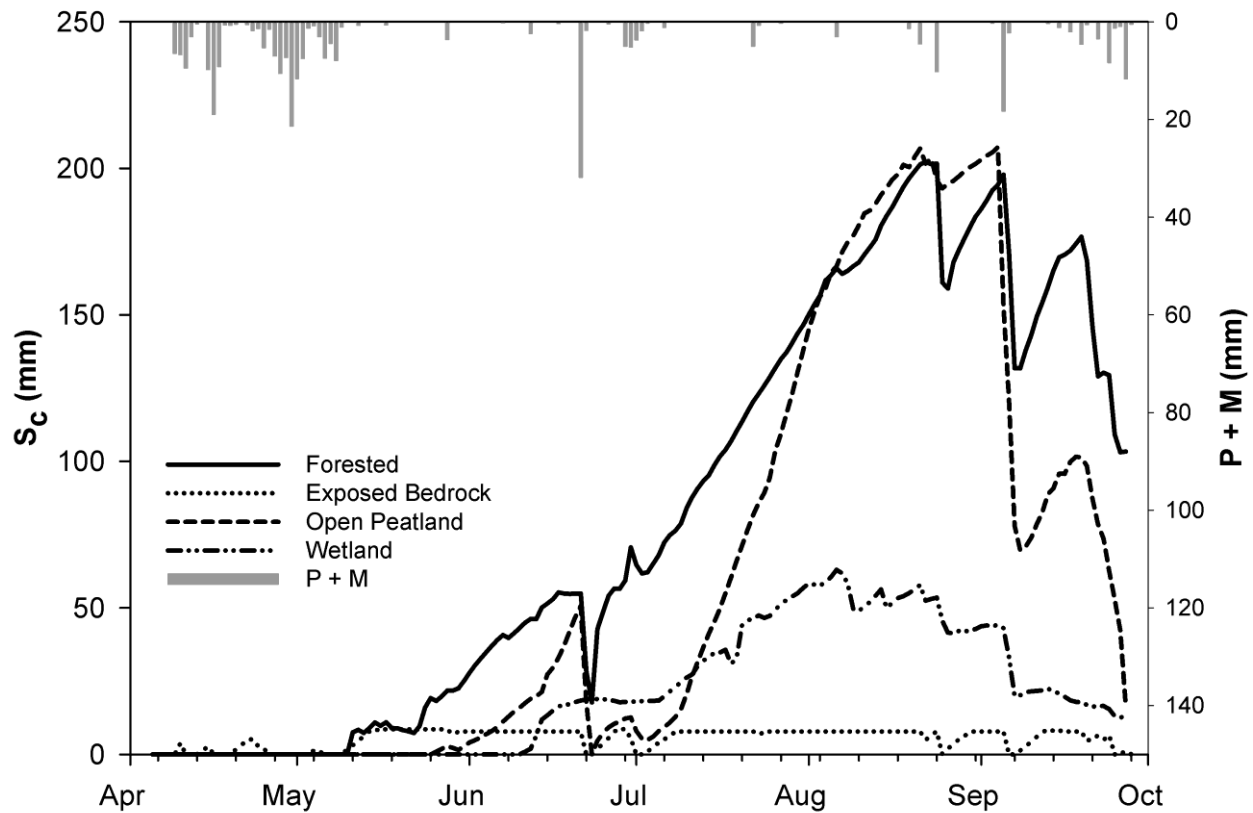


Figure 5.2: Storage capacity,  $S_c$ , for terrestrial land covers as well as rainfall,  $P$ , and snowmelt,  $M$ , inputs during 2009.  $P$  and  $M$  presented in this plot are for the Baker Creek Research Basin as a whole. Although rainfall is variable throughout the basin, the plot presented here serves as a valid approximation of the magnitude and timing of inputs to the three study basins.



Table 5.1: Observed active area,  $A_a$ , contributing area,  $A_c$ , overall connectivity of the stream network,  $C_{E,N}$ , and connectivity of the stream network to the outlet,  $C_{E,O}$ .

Date	Trail Creek				Eagle Pass Creek				Duckfish Lake			
	09-May	17-May	20-Jun	27-Aug	09-May	17-May	20-Jun	27-Aug	09-May	17-May	20-Jun	27-Aug
$A_a$ ( $m^2 \times 10^6$ )	7.84	2.75	0.44	0.36	20.66	8.58	3.17	2.90	25.16	14.13	9.74	8.49
$A_c$ ( $m^2 \times 10^6$ )	7.84	2.18	0.01	0.01	20.66	7.07	2.40	2.03	25.16	12.21	8.19	7.92
$C_{E,N}$	1.00	1.00	0.69	0.73	1.00	0.99	0.80	0.81	1.00	0.99	0.77	0.51
$C_{E,O}$	1.00	1.00	0.01	0.03	1.00	0.98	0.43	0.36	1.00	0.97	0.40	0.31

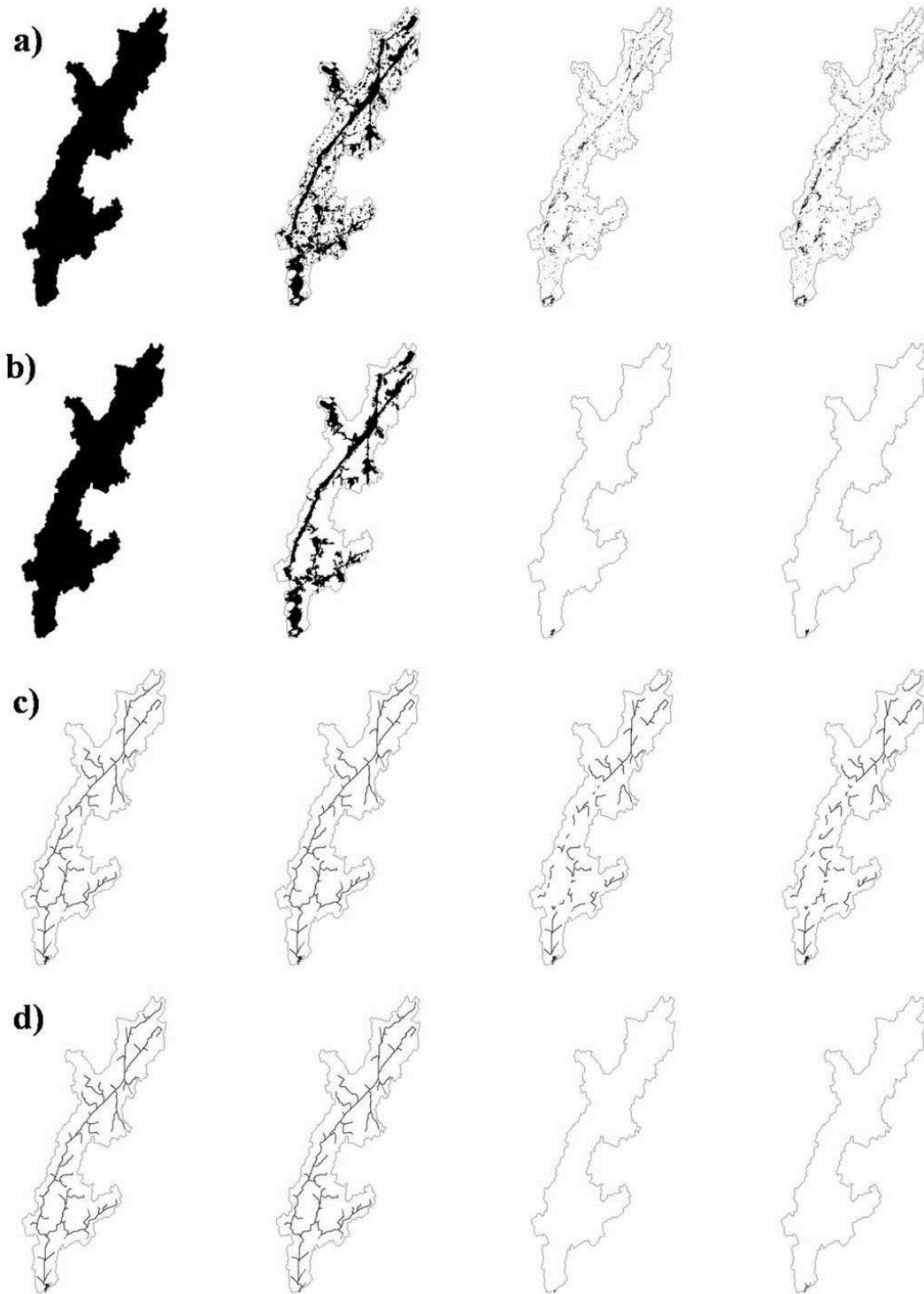


Figure 5.3: Trail Creek active area (a), contributing area (b), active stream network (c), and contributing stream network (d) for (from left to right) May 9, May 17, June 20, and August 27, 2009.

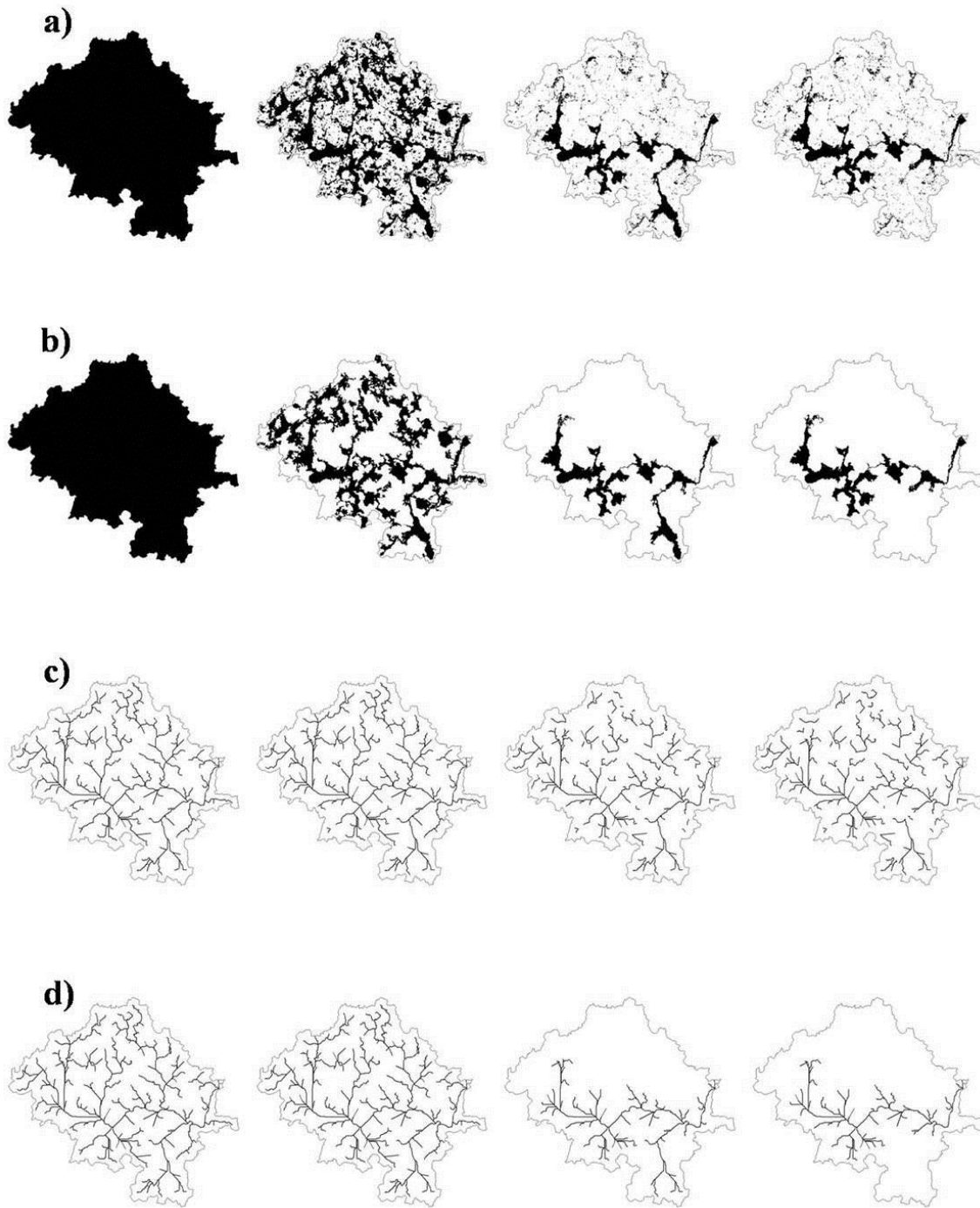


Figure 5.4: Eagle Pass Creek active area (a), contributing area (b), active stream network (c), and contributing stream network (d) for (from left to right) May 9, May 17, June 20, and August 27, 2009.

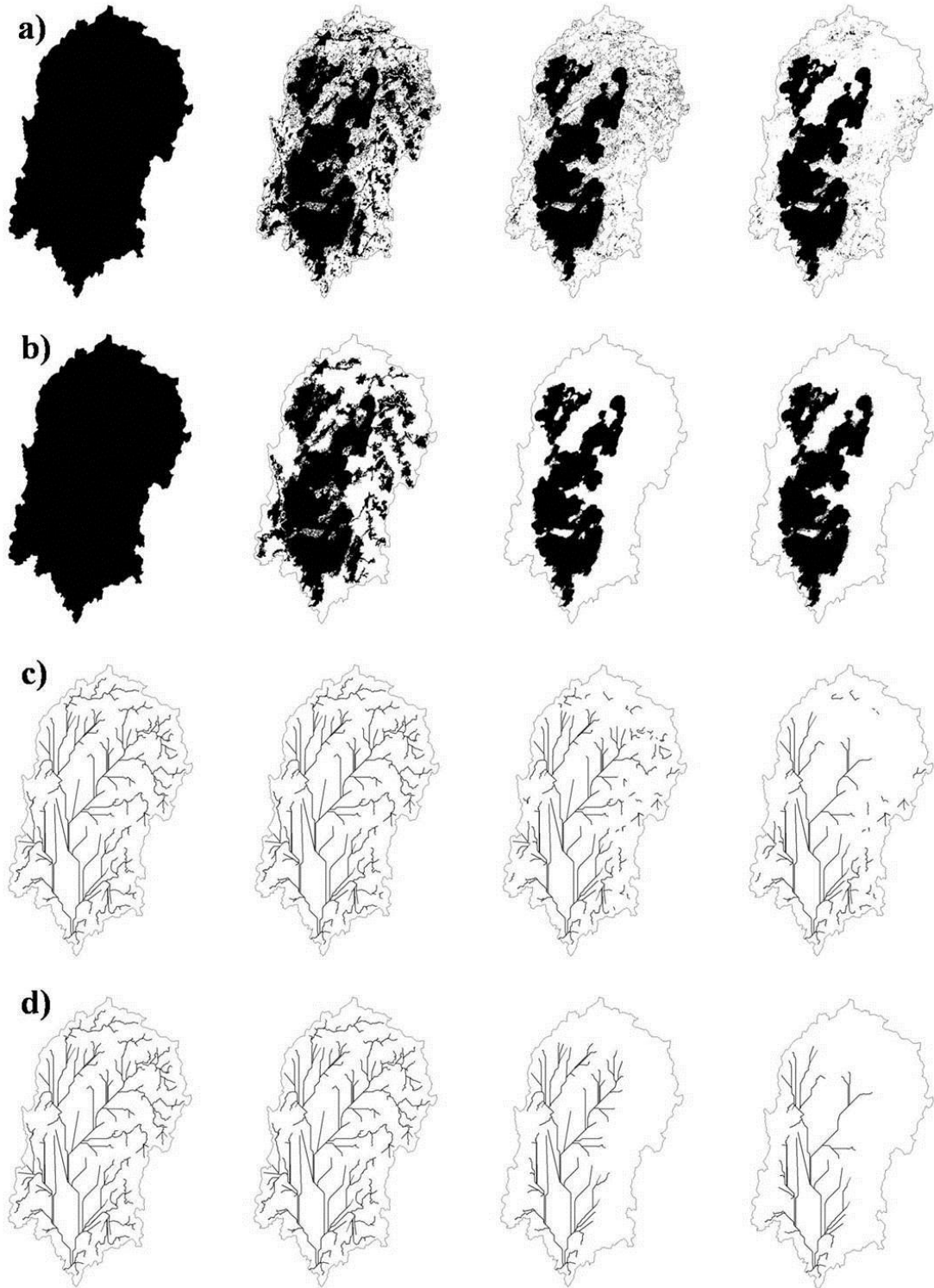


Figure 5.5: Baker Creek below Duckfish Lake active area (a), contributing area (b), active stream network (c), and contributing stream network (d) for (from left to right) May 9, May 17, June 20, and August 27, 2009.

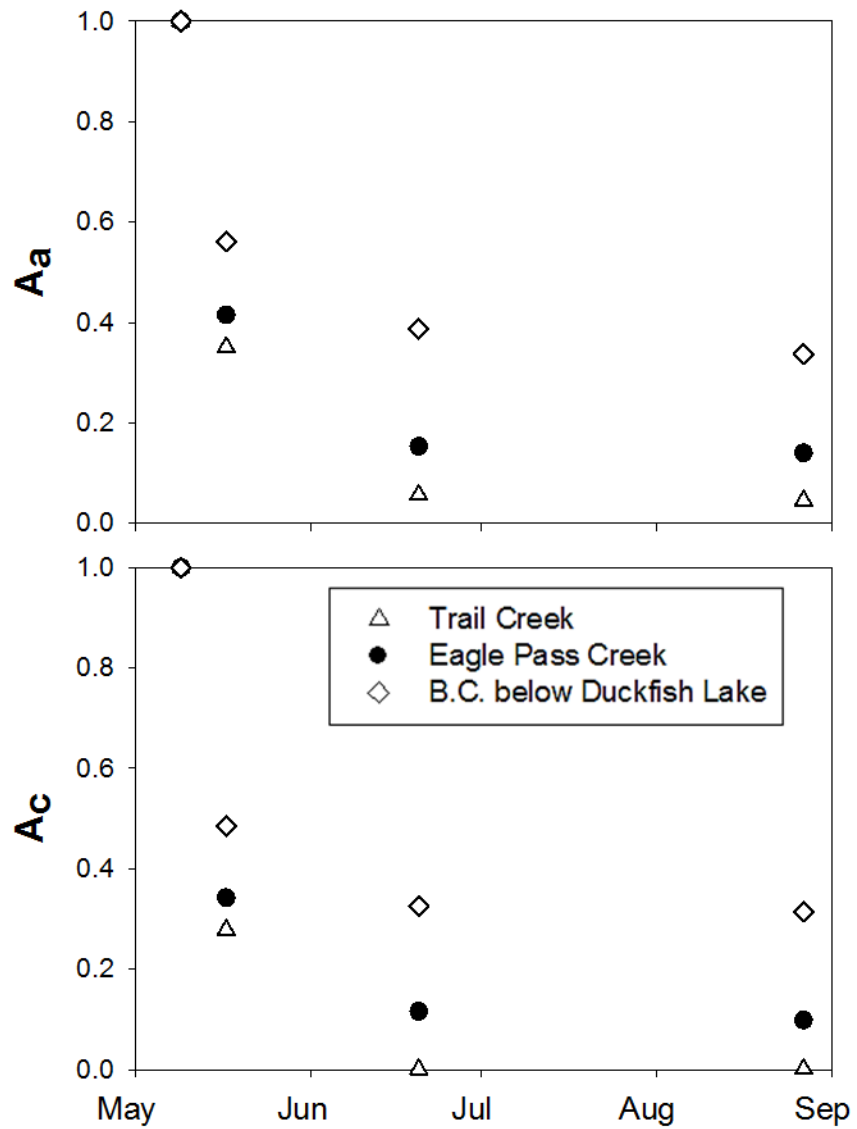


Figure 5.6: Active area,  $A_a$  (top), and contributing area,  $A_c$  (bottom), in the three study basins for the days listed in Table 3.2. In the figure above active area and contributing area are presented as percentages of gross drainage area to facilitate comparison.

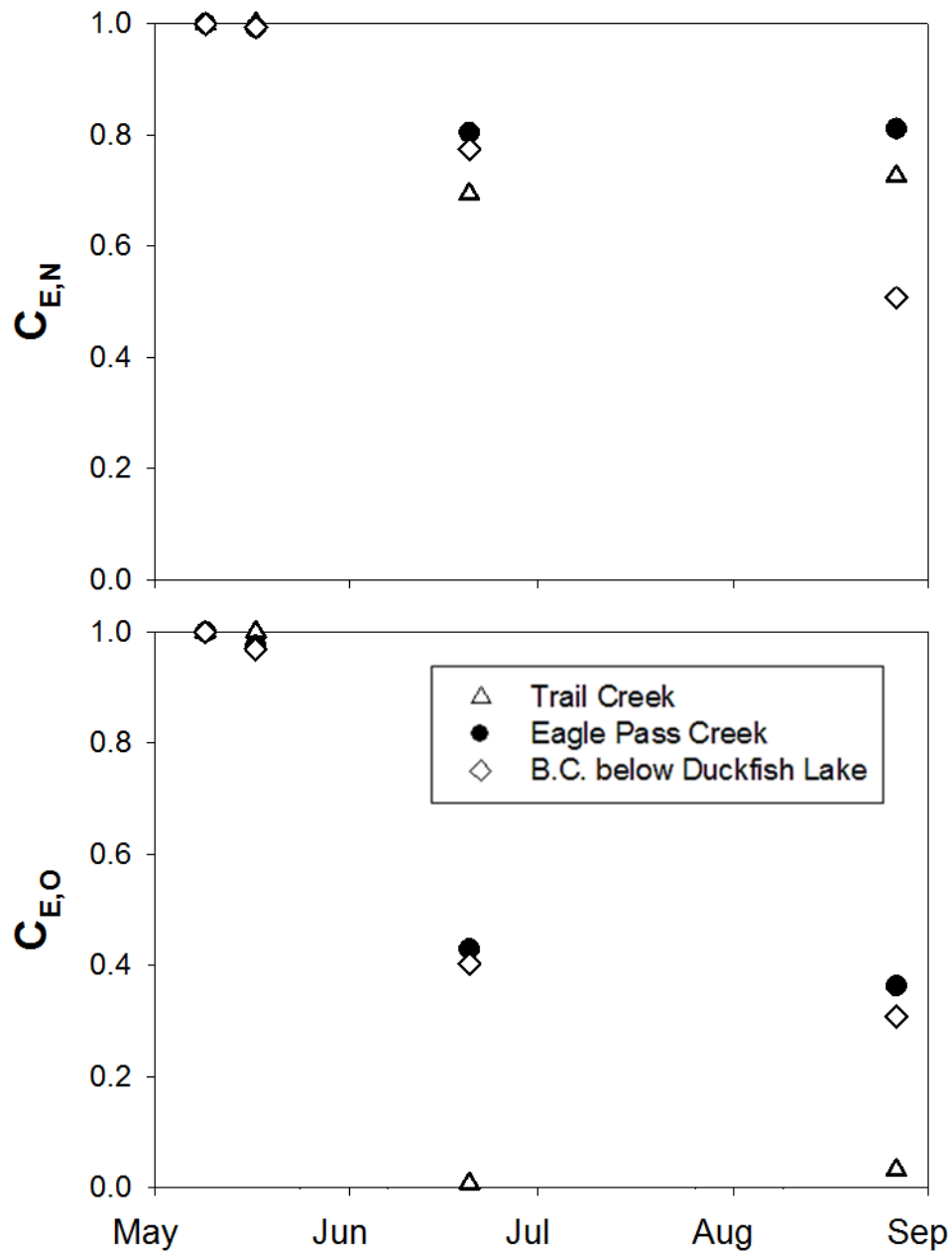


Figure 5.7: Overall stream network connectivity,  $C_{E,N}$  (top), and connectivity of the stream network to the outlet,  $C_{E,O}$  (bottom), in the three study basins for the days listed in Table 3.2. The May 9, 2009 and May 17, 2009 values were very similar for most sub-basins.

Rainfall before June 20 was light (12 mm) and losses to evapotranspiration and runoff caused an increase in  $S_c$  for all land covers (Figure 5.2). Peatlands became inactive on May 27 and wetlands on June 11 (Figure 5.2). Open peatland and wetland land covers were not completely inundated but partial surface ponding was still regionally prolific and was captured through remote sensing (Figures 5.3-5.5). Storage capacity in key terrestrial elements such as peatlands (Figure 5.2) resulted in the widespread disconnection of headwater terrestrial sub-catchments from the lake modulated stream network (Figures 5.3-5.5) and inputs to headwater lakes slowed. On June 14, small headwater lakes began to disconnect. The lack of inflows to receiving lakes following the disconnection of headwater lakes upstream meant that evaporation and outflow quickly reduced the remaining detention storage and the lake modulated stream network quickly disintegrated. By June 20  $C_{E,N}$  and  $C_{E,O}$  had dropped significantly (Figures 5.3-5.5 and 5.7). In the Trail Creek sub-basin, unlike the peatlands, the channel wetlands between receiving lakes remained inundated and active (Figure 5.3). However, lakes with levels below their outlet elevation caused the disintegration of the stream network (Figure 5.3) and  $A_c$  decreased to a minor wetland immediately upstream of the gauge site (Figures 5.3 and 5.6, Table 5.1). However, large headwater lakes with high volumes of detention storage and inefficient outlets were able to maintain outflow. In the central lake chain of the Eagle Pass Creek sub-basin, connectivity to the outlet was maintained throughout the summer by outflow contributed from Snowf Lake (not official name) and a large wetland complex on its north western shore (Figures 3.1 and 5.4). The rest of the Eagle Pass Creek sub-basin was disconnected from the outlet by headwater lakes (Figure 5.4). However, saturated portions of open peatlands upstream of these headwater lakes (Figure 5.4) kept  $C_{E,N}$  higher than in the other two study basins by maintaining the connectivity of upland sub-catchments on June 21 and August 27, 2009 (Figure 5.7, Table

5.1). In the Duckfish Lake sub-basin, the large peatland and wetland complexes in the northeast of the sub-basin (Figure 3.1) became inactive and disconnected outlying areas from the outlet (Figure 5.5). The contributing stream network was limited to Duckfish Lake and its surrounding shoreline (Figure 5.5 and 5.7).

A rainfall of 34 mm fell on June 23 and was sufficient to fill the  $S_c$  of exposed bedrock, open peatlands and both headwater and receiving lakes (Figure 5.2). The stream network re-integrated starting with headwater terrestrial sub-catchments in which bedrock was dominant and where reactivated peatlands permitted water to cascade downstream to the drainage network's core lake chains. The runoff driven flood wave re-established the connectivity of the stream network and resulted in a streamflow response at each outlet (Figure 5.1). Through July and August,  $S_c$  increased in all terrestrial land covers (Figure 5.2) and inactive lakes due to evapotranspiration exceeding precipitation. On August 27, the active stream network remained largely disconnected (Figure 5.3-5.5) and  $C_{E,O}$  was low (Figure 5.7). The state of the terrestrial land covers was generally inactive and all lakes except for those downstream of Duckfish Lake and Snowf Lake were inactive (Figures 5.3-5.5). A rainfall of 21 mm on September 6 filled  $S_c$  in the exposed bedrock and reduced it in other land covers (Figure 5.2). The September 6 rainfall event was insufficient to re-establish the lake modulated stream network and stream flow response was minimal in all sub-basins except Eagle Pass Creek (Figure 5.1). As the instrumentation was removed at the end of September, a succession of smaller rain events was gradually filling  $S_c$  in all terrestrial land covers (Figure 5.2).



### 5.3 Contributing stream network and contributing area

As contributing area contracted (Figures 5.3-5.5 and 5.6), the contributing stream network that it was able to support followed (Figure 5.8). Figure 5.8 shows the observed relationship between the contributing area and contributing stream length as well as the relationship observed between the contributing area and length of the longest contributing stream both plotted on a double log plot. The length of contributing streams appeared to be higher for a given contributing area when the hydrograph was in recession rather than when the hydrograph was rising.

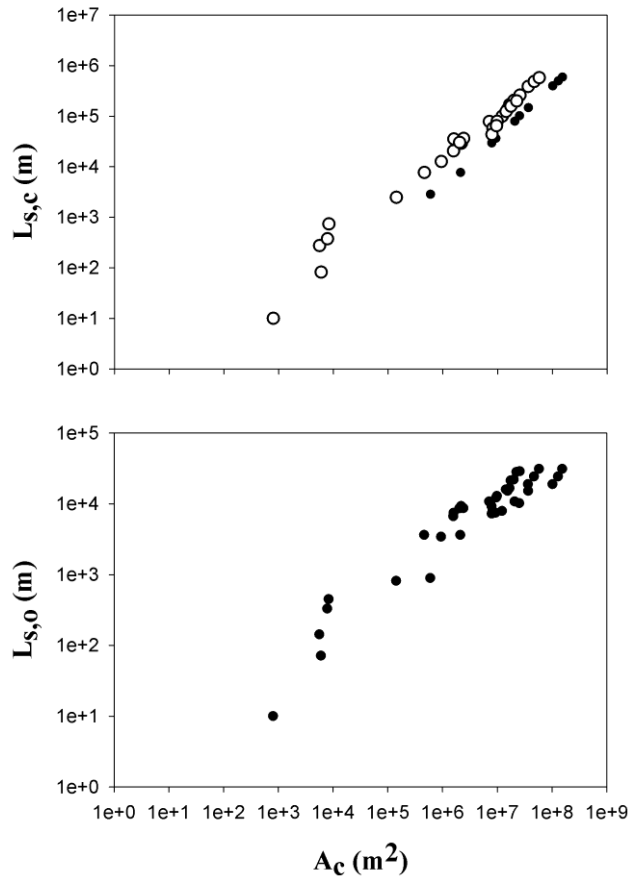


Figure 5.8: Plot relating contributing stream length,  $L_{s,c}$ , to contributing area,  $A_c$ , (top) and the length of the longest contributing stream,  $L_{s,o}$ , and contributing area (bottom) Baker Creek as a whole and nine of its sub-basins. In the plot of  $L_{s,c}$  vs.  $A_c$  the values while the hydrograph was in recession are marked by white circles and the values while the hydrograph was rising are marked by black circles. Both figures are plotted on a log vs. log scale.

#### 5.4 Connectivity and streamflow

Between May 9 and May 17, connectivity remained high in all three study basins. Over this period flow increased at the outlet of Eagle Pass Creek and Baker Creek below Duckfish Lake while decreasing slightly at the outlet of Trail Creek. Through the summer, the stream network disintegrated and  $C_{E,O}$  decreased (Figures 5.3-5.5 and 5.7). As the contributing stream network contracted (Figure 5.3-5.5), the area able to contribute decreased and  $Q$  at the outlet fell. There was a general positive relationship between  $C_{E,O}$  and  $Q$  (Figure 5.9). However, the nature of the relationship between  $C_{E,O}$  and  $Q$  was observed to be different for each sub-basin (Figure 5.9). Trail Creek was observed to be either highly or poorly connected to its outlet. When  $C_{E,O}$  was 1.0 on May 17, flow was  $0.08 \text{ m}^3 \cdot \text{s}^{-1}$ . When poorly connected,  $C_{E,O}$  was less than 0.03 and  $Q$  was less than  $0.015 \text{ m}^3 \cdot \text{s}^{-1}$ . Streamflow at the outlet of Eagle Pass Creek was observed to decrease from the high flow in May with a roughly logarithmic relationship to decreases in  $C_{E,O}$  (Figure 5.9). At Duckfish Lake,  $C_{E,O}$  dropped from 0.98 to 0.40 from May 17 to June 20 but  $Q$  only decreased from  $0.17 \text{ m}^3 \cdot \text{s}^{-1}$  to  $0.13 \text{ m}^3 \cdot \text{s}^{-1}$ . From June 20 to August 27,  $C_{E,O}$  decreased from 0.40 to 0.31 but over the same period a decrease in  $Q$  from  $0.13 \text{ m}^3 \cdot \text{s}^{-1}$  to  $0.04 \text{ m}^3 \cdot \text{s}^{-1}$  was observed. As a result the relationship between  $C_{E,O}$  and  $Q$  follows a logarithmic form.

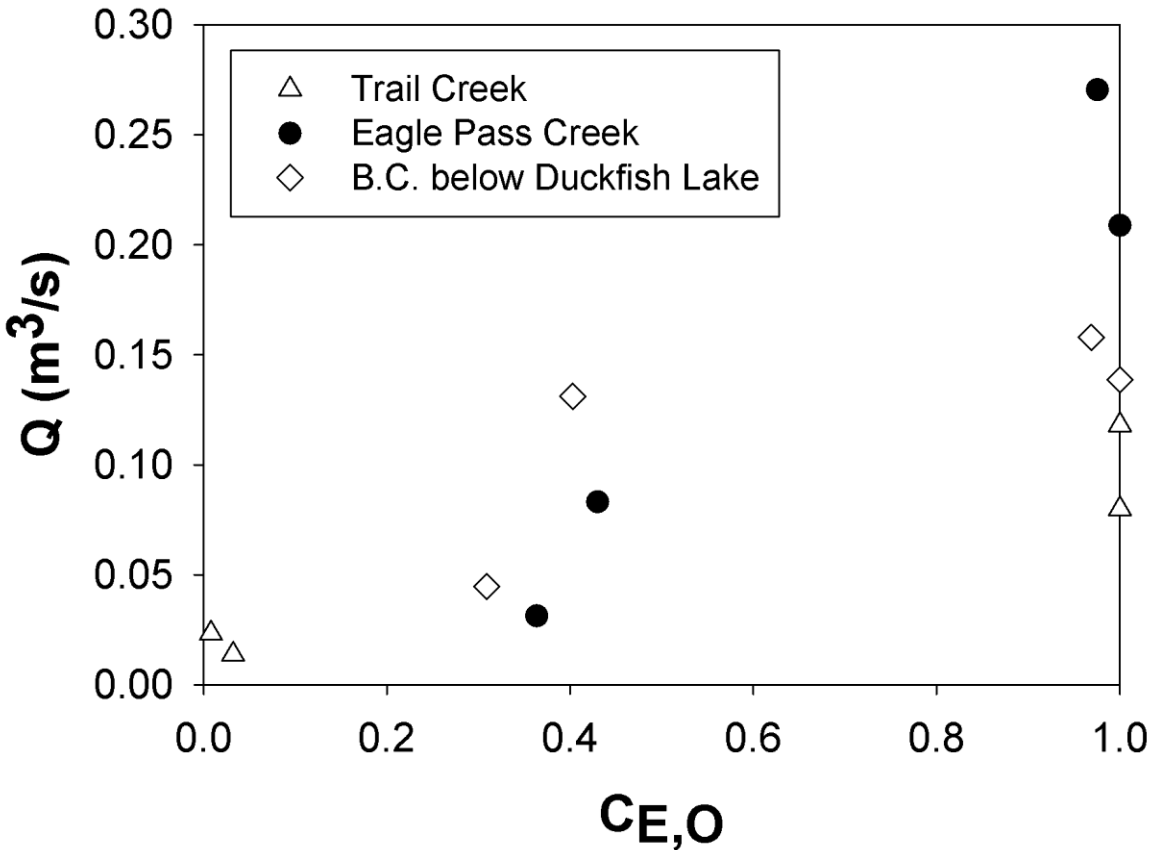


Figure 5.9: Daily average streamflow,  $Q$  ( $m^3 \cdot s^{-1}$ ), on the satellite image acquisition date defined in Table 3.2, for different states connectivity to the outlet,  $C_{E,O}$ , in the sub-basins of interest.

### 5.5 Connectivity and runoff response

Responses to rainfall and melt events were examined relative to antecedent connectivity in each study basin (Figure 5.10, Table 5.2). On May 19 when  $C_{E,O}$  was high, a small melt event produced a response in all sub-basins that were already in recession. The slope of the recession was altered at Trail Lake yielding a  $Q_e$  of  $816 \text{ m}^3$  with a  $R_r$  of 0.68. In the Eagle Pass sub-basin, the melt increased flow for two days yielding a  $Q_e$  of  $11,844 \text{ m}^3$  with a  $R_r$  of 0.53. Baker Creek below Duckfish Lake responded to an input of  $15,099 \text{ m}^3$  with a  $Q_e$  of  $4,727 \text{ m}^3$  and with a  $R_r$  of 0.32. On June 23 a rainfall event of 34 mm occurred. Although prior to the rain event  $C_{E,O}$  was

low (Figure 5.7),  $S_c$  was still relatively small, especially in lakes which had recently disconnected. During the June 23 event, Trail Creek sub-basin received 243,758 m<sup>3</sup> and yielded 36,667 m<sup>3</sup> with a  $R_r$  of 0.15. Eagle Pass Creek sub-basin received 741,810 m<sup>3</sup> resulting in a  $Q_e$  of 70,187 m<sup>3</sup> with a  $R_r$  of 0.09. The Baker Creek below Duckfish Lake sub-basin received 770,037 m<sup>3</sup> and yielded 50,960 m<sup>3</sup> with a  $R_r$  of 0.07. On September 6, a rainfall event of 21 mm occurred. With the exception of the bedrock, the terrestrial land covers remained inactive during the rain event and contribution to storm flow was limited to lake chains connected to the outlet and their adjacent bedrock lake shores. The 88,568 m<sup>3</sup> of rainfall on the Trail Creek sub-basin produced a  $Q_e$  of only 2,313 m<sup>3</sup> with a  $R_r$  of 0.01. On September 6, 456,658 m<sup>3</sup> of rain fell on the Eagle Pass sub-basin yielding a  $Q_e$  of 26,514 m<sup>3</sup> with a  $R_r$  of 0.06. The Baker Creek below Duckfish Lake sub-basin received 415,216 m<sup>3</sup> of rain and yielded a  $Q_e$  of 4,343 m<sup>3</sup> with a  $R_r$  of 0.01.

Table 5.2: Runoff characteristics observed for rainfall or melt events following satellite image acquisition during 2009

Date	P or M (m <sup>3</sup> )			Q <sub>e</sub> (m <sup>3</sup> )			R <sub>r</sub>		
	Trail	Eagle Pass	Duckfish	Trail	Eagle Pass	Duckfish	Trail	Eagle Pass	Duckfish
<b>19-May-09</b>	1,568	22,730	15,099	816	11,844	4,727	0.68	0.53	0.32
<b>23-Jun-09</b>	243,758	741,810	770,037	36,667	70,187	50,960	0.15	0.09	0.07
<b>06-Sep-09</b>	88,568	456,658	415,216	2,313	26,514	4,343	0.01	0.06	0.01

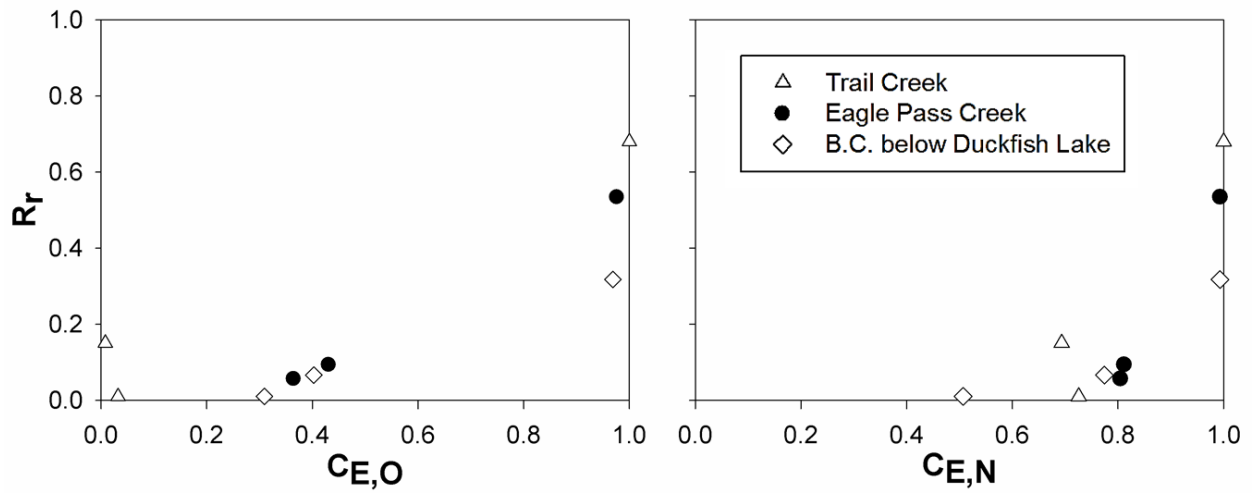


Figure 5.10: Runoff ratios,  $R_r$ , observed for different antecedent states of connectivity of the stream network to the outlet,  $C_{E,O}$  (left), and overall connectivity of the stream network,  $C_{E,N}$  (right).

## CHAPTER 6: DISCUSSION

### 6.1 Connectivity dynamics

Storage states were highly dynamic and all land cover types were observed to be capable of operating as runoff sources or sinks. For a brief period in early May, all sub-catchments were connected downstream and functioned as sources. The stream network then disintegrated as individual elements became inactive and disrupted the connectivity of the stream network. As the stream network disintegrated, it was segmented into one component connected to the outlet and one or more internally drained components that were active but not connected to the outlet. This caused the divergence of  $A_c$  and  $A_a$  (Figure 5.6) as well as  $C_{E,N}$  and  $C_{E,O}$  (Figure 5.7) after May 17.

Black (1997) proposed that basins could perform collecting, storing, and discharging functions. It was observed that individual elements could perform these same functions. The function of individual elements that collected and attenuated runoff was observed to drive the dynamics of basin scale connectivity. When active, they could perform all three functions, when inactive they could only collect and store. These elements modulated connectivity by acting as “*gatekeepers*” for upstream contributing areas. At Baker Creek, the open peatlands and wetlands situated in upland areas modulated the connectivity of bedrock dominated headwater catchments. Downstream, lakes were gatekeepers for large tracts of headwater sub-catchments.

When active, gatekeepers facilitate the transfer of runoff contributed from headwaters both by remaining active themselves as well as maintaining the connectivity of the stream network downstream. They do so by attenuating runoff collected from upstream, storing it and slowly releasing it over time and sustaining streams downstream that would otherwise run dry. A gatekeeper's ability to remain active depends on its size and efficiency (Spence, 2007) in translating stored runoff collected from upstream to outflow as well as the intensity and duration of upstream contributions. The intensity and duration of upstream contributions to gatekeeper headwater lakes has been noted to be heavily influenced by the land cover in the areas upstream as well as the size of the lake relative to the gross drainage area upstream (Mielko and Woo, 2006). Gatekeeper elements with large volumes and relatively inefficient outlets such as Duckfish Lake were able to remain active longer by attenuating large volumes of spring snowmelt. Gatekeeper elements located further downstream in the stream network were able to remain active longer as the duration of runoff collection from upstream was prolonged. For instance at Eagle Pass Creek, small receiving lakes located downstream of Snowf Lake (Figures 3.1 and 5.4) were maintained by outflow through the summer months and remained active long after headwater lakes of comparable size (Figure 5.4) had disconnected. The effect of a gatekeeper on  $C_{E,O}$  downstream is controlled by its topology and by the rate and duration of outflow. Snowf Lake, located in the headwaters of Eagle Pass Creek, maintained lake levels and connectivity downstream from June until September.

When inactive, gatekeeper elements disrupt connectivity and act as sinks for contributions from upstream. The area of a gatekeeper influences the amount of run-on required from upstream to become active. Storage capacity is proportional to surface area, and therefore the larger a

gatekeeper is, the greater the input volume required to re-establish connection. The topology of a gatekeeper defines the impact that its inactivity may have on  $C_{E,O}$ . The influence of a gatekeeper element on  $C_{E,O}$  increases the further downstream it is located. With closer proximity to the outlet, its inactivity disconnects potential contributions from an increasing number of upstream elements.

It is important to note that as upstream areas disconnect, the relative topology of downstream elements changes. As the stream network upstream became disconnected (Figures 4-6), downstream elements reverted to performing “headwater” functions. This dynamic relative topology resulted in a cascading effect of disconnection; regions dominated by headwater terrestrial catchments with small efficient gatekeepers quickly disintegrated during hydrograph recession. This was particularly pronounced in the Trail Creek basin where small and efficient gatekeeper peatlands and lakes (Figure 3.1) caused a highly variable connectivity and highly ephemeral streamflows (Figures 5.1, 5.3, and 5.7). This also caused the rapid disconnection of terrestrial portions outlying from the central Eagle Pass Creek lake chain (Figure 5.4) and Duckfish Lake (Figure 5.5).

## **6.2 Contributing stream length and contributing area**

As the contributing area contracted, the cumulative length of the contributing stream network decreased according to a power relationship (Figure 5.8). Power relationships abound in the hydrology of drainage networks and often possess scaling invariance (Rodriguez-Iturbe and Rinaldo, 1997). The relationship between the longest contributing stream, measured from the outlet to the furthest upstream contributing stream, and contributing area appears to be a



variation of the geomorphological law that was first developed by Hack (1957) and affirmed and refined by further studies (Gray, 1961; Muller, 1973; Rigon et al., 1996). In Hack's Law relationships, the length of the longest stream measured from the divide to the outlet is a function of basin area,  $A$  ( $m^2$ ), raised to the power of an exponent of  $h \approx 0.6$  (Rodriguez-Iturbe and Rinaldo, 1997).

$$L \propto A^h \quad (17)$$

In this study, the law was found to hold for variable contributing areas and the longest contributing stream they were able to support and had  $r^2=0.92$ .

$$L_{s,o} = 0.630 \cdot A_c^{0.605} \quad (18)$$

The Hack's Law observed here is consistent with fractality as the elongation exponent, 0.18, was observed to be greater than 0 (Rodriguez-Iturbe and Valdes, 1997). This implies that the Hack's Law relationship observed here for the longest contributing stream and contributing area is independent of scale.

A power relationship was also observed for the length of the contributing stream network and contributing area with  $r^2=0.96$ .

$$L_{s,c} = 0.086 \cdot A_c^{0.851} \quad (19)$$

This power relationship exists because a dendritic network is less centralized and has a higher drainage density in its headwaters than further downstream. As a result the cumulative length of contributing streams increases more with the connection of the headwaters than the core lake chain. The contributing stream length sustained by a given contributing area during the rising limb and the receding limb of the hydrograph appear to be distinct from one another and allude to a certain degree of hysteresis in the relationship between  $L_{s,c}$  and  $A_c$  (Figure 5.7). Such

hysteresis would emerge because higher order gatekeepers have a more significant control on the contributing stream length than similar lower order elements situated in the headwaters. Due to the increased duration and intensity of upstream contributions collected by higher order elements, the volume they store is larger than similar lower order gatekeepers and they can slowly discharge attenuated storage after contributions from upstream cease. As a result, stream length downstream of large and persistent gatekeepers can remain relatively unchanged while contributing area contracts so long as gatekeepers remain active and discharging stored water that had been previously collected from the headwater terrestrial areas.

### **6.3 Connectivity and streamflow**

At high connectivity, there was a high range of streamflow values observed for each basin. At Trail Creek,  $C_{E,O}$  remained at 1 while flow at its outlet receded between May 9 and May 17. Flows in both Eagle Pass Creek and Baker Creek below Duckfish Lake were still rising on May 9 and although connectivity dropped slightly between May 9 and May 17 streamflow increased. This was the result of the simultaneous disconnection of headwater terrestrial areas and advance of the main spring freshet flood wave downstream. This showed that a highly connected stream network can support a range of flow, and alludes to the potential for a possible hysteretic relationship between connectivity and streamflow. Hysteretic relationships have long been noted in hydrology especially in looped rating curves (Chow et al., 1988), in relationships between soil tension and soil water content, and have recently been noted by Spence et al. (2010) in relationships between basin storage and contributing area. In each case, the hysteresis emerges because the dependant variable is not dependant solely on the independent variable and usually depends on a lag or memory within the system. As a result there is not one unique dependant

value of the dependant variable, it depends on whether or not the system is in a phase of becoming wetter or becoming drier.

After May 17, decreasing values of  $C_{E,O}$  resulted in lower  $Q$  in the three study basins (Figure 5.9). However, the characteristic shape of relationships observed between  $Q$  and  $C_{E,O}$  varied significantly for each sub-basin. The characteristic shape of the relationship between  $C_{E,O}$  and  $Q$  was greatly influenced by the configuration and size of active areas in the stream network and relationships between storage and discharge within individual elements. At the basin scale, the active areas of particular importance to  $Q$  were lakes. In a drainage basin where the last store in the chain was small relative to upstream contributions, inflows from the contributing stream network heavily influenced lake detention storage in the outlet controlling lake and thus sub-basin outflow. For instance, Trail Lake was small relative to its upstream contributing area and did not significantly attenuate outflow. Inflows from the contributing stream network heavily influenced lake detention storage and thus sub-basin outflow. When upstream contributions were high as they were on May 17, connectivity and flow were high. However, when connectivity was low as it typically was in summer, streamflow in the Trail Creek sub-basin was minimal (Figures 5.3 and 5.9). At Eagle Pass, lakes of similar size were distributed throughout the central lake chain and headwaters. The relationship between  $C_{E,O}$  and  $Q$  at Eagle Pass was roughly logarithmic with the steepest slope of the three study basins. The headwater lakes that collect water from the hillslopes in Eagle Pass were still connected on May 17 and streamflow was high. By June 20 many of the headwater lakes outlying from the central chain had become disconnected and flow significantly decreased. Although one more lake in the south of the basin became disconnected, connectivity remained stable after June 20 and  $Q$  decreased as detention storage in the central lake chain was exhausted due to evapotranspiration and outflow. Because

the lakes are all small in Eagle Pass Creek (Figure 3.1 and Table 3.1), no individual lake exerted exceptional influence on the streamflow close to the outlet of the sub-basin. This was not the case for lakes that are large relative to their upstream contributions and situated close to the basin outlet. Such lakes exerted significant influence on the basin outflow and dampened any influence of upstream connectivity. This was observed at the Baker Creek below Duckfish Lake sub-basin in particular, where Duckfish Lake controlled basin outflow and caused a logarithmic relationship between  $Q$  and  $C_{E,O}$ . This resulted from the fact that after June 20, the contributing portion of Baker Creek below Duckfish Lake remained stable and confined to Duckfish Lake itself and a few terrestrial sub-catchments lining its shores (Figure 5.5) but the level of Duckfish Lake had dropped significantly over the same period. Because of its location and relative size, the level and stage-discharge relationship of Duckfish Lake were the primary controls on outflow from the Baker Creek below Duckfish Lake sub-basin and so,  $C_{E,O}$  had little influence on  $Q$ .

#### **6.4 Connectivity and runoff response**

Generally, higher antecedent connectivity was found to result in higher  $R_r$  (Figure 5.10). On May 19, antecedent connectivity was high and even small inputs were translated to streamflow at the outlet with relatively high efficiency (Figure 5.10 and Table 5.1). When antecedent connectivity was low, rainfall was first directed to fill storage capacities and re-establish inactive connections before reaching the outlet. However, the relationships between runoff response and connectivity differed for each sub-basin and the emergence and magnitude of runoff response was punctuated by the importance of the magnitude of inputs relative to antecedent storage capacities in the drainage network's gatekeeper elements. Input events large enough to re-establish the connectivity of the stream network to the outlet by reactivating gatekeepers induced

a streamflow response. In flashy basins (e.g. Trail Creek) ample source areas and small inactive gatekeeper elements meant that runoff response could be highly variable even when antecedent connectivity and streamflow were low. Once the bedrock areas were active, storage capacities in the relatively small gatekeeper peatlands and lakes downstream were quickly filled: the June 23 rain event was large enough to activate the bedrock, then gatekeeper peatlands and lakes so that flow in Trail Creek rose disproportionately to the antecedent connectivity (Figure 5.10 and Table 5.1). Input events that were not large enough to re-establish connectivity to the outlet did not produce a streamflow response. Smaller rain events (e.g. September 6) only activated areas with small  $S_c$  but were not large enough to activate gatekeepers (Figure 5.2), so little or no response was observed at the outlet (Figures 5.1 and 5.10, Table 5.1). The runoff response curves were shaped by the relative efficiency of different portions of the drainage network in producing runoff from inputs. In Figure 5.10, values of  $C_{E,O}$  approaching 1 are associated with connections in the headwaters of the drainage network, values closer to 0 are associated with connections in the central lake chains of the drainage network. In Eagle Pass, the relationship between  $R_f$  and  $C_{E,O}$  was roughly linear and thus additional elements from the expanding contributing stream network were equally efficient at translating rainfall to runoff. This results from the distribution of small lakes of similar size throughout the drainage network that control the connectivity of the stream network. At Duckfish Lake, the relationship between  $C_{E,O}$  and  $R_f$  was nearly linear but the slope of the relationship was less steep than that observed for Eagle Pass. This is likely because the influence of the headwater connections was obscured by Duckfish Lake which controlled flow out of the basin. The presence of such an element at the outlet of the basin decreases efficiency by attenuating runoff longer, prolonging the duration of the runoff event and enabling more collected runoff to be abstracted by evapotranspiration while being transmitted to

the outlet.

In Figure 5.10, values of antecedent  $C_{E,N}$  closer to 1 can be associated with connections from areas whose activity is not persistent such as headwater terrestrial sub-catchments dominated by bedrock and small gatekeeper elements, lower values of antecedent  $C_{E,N}$  can be associated with elements whose inactivity is less likely. At Trail Creek, the relationship between  $R_r$  and  $C_{E,N}$  shared a highly variable pattern similar to that noted between  $R_r$  and  $C_{E,O}$ . In distributed sub-basins where most of the inactive gatekeepers were of similar size and small like Eagle Pass, less persistent gatekeepers had a similar influence on  $R_r$  as more persistent ones and the increase in  $R_r$  with higher  $C_{E,N}$  was nearly linear (Figure 5.10). In the Baker Creek below Duckfish Lake sub-basin, the relationship between  $R_r$  and  $C_{E,O}$  was notably non-linear and the activity of the less persistent connections induced a greater increase in  $R_r$  than the more persistent connections. This implies that the less persistent elements in the headwaters are more efficient than Duckfish Lake at translating inputs to runoff. This relative efficiency of headwater terrestrial portions stems from the fact that the transmission of collected runoff is distributed among a large number of small gatekeepers with efficient outlets over a landscape with greater relief than further downstream. The relative inefficiency of Duckfish Lake results from the abstraction by evaporation of large volumes of collected runoff while it is stored and slowly translated to discharge through Duckfish Lake's single and relatively inefficient outlet.

### **6.5 Basin classification based on the influence of connectivity on runoff response**

For a particular drainage basin the influence hydrological connectivity has on runoff response is controlled by four traits: 1) the efficiency of headwater source areas, 2) the proportion of

headwater source areas, 3) the efficiency and size of gatekeepers relative to upstream contributions, 4) the ability of gatekeepers to attenuate flow. Climate would also presumably affect the influence of connectivity by dictating the magnitude, frequency, and duration of inputs to the basin. Variations in inputs could not be analyzed in this study with the basins in such proximity to one another. Figure 6.1 summarizes the influence that heterogeneity can have on the relationship between connectivity and runoff response. At one end of the spectrum are basins with a high proportion of efficient headwater source areas and small, efficient but non-persistent gatekeepers, which exhibit a flashy runoff response and a poor relationship between connectivity and runoff response. At the other end of the spectrum are basins with efficient headwaters and large, inefficient, persistent gatekeepers. The runoff response from such basins is attenuated and the influence of connectivity on runoff response is non-linear. In the middle are basins with a high proportion of efficient source areas in the headwaters, and small, efficient but persistent gatekeepers, which will have a characteristically regular runoff responses and the relationship between connectivity and runoff response would be linear.

Table 6.1: Basin classification according to the influence of connectivity on runoff response.

	<i>Influence of hydrological connectivity on runoff response</i>		
	←	→	→
Characteristic runoff response	Flashy	Regular	Attenuating
$C_{E,O}$	Highly variable	Linear	Linear
$C_{E,N}$	Highly variable	Linear	Non-linear
Land cover traits	Efficient headwaters and small, efficient, non-persistent gatekeepers	Efficient headwaters and small, efficient, persistent gatekeepers	Efficient headwaters and large, inefficient, persistent gatekeepers

## **6.6 Discussion of Limitations and Recommendations**

This thesis is an initial exercise in the quantitative investigation of connectivity and provides insight into connectivity dynamics in a heterogeneous drainage basin as well as the influence that the connectivity of the stream network has on streamflow and runoff response. However, its scope of application has limits and improvements to methods and approach are recommended in future work. In this study, the dates of analysis were limited to the optical satellite imagery acquisition dates. Accordingly, the results were limited to looking at basin scale connectivity as an antecedent condition. Connectivity at the basin scale is dynamic and a more comprehensive study would account for changes to connectivity in real time. An improved application could establish connectivity on a single day and move forward in time using measured or modeled hydrological process variables and water budget terms. This would provide greater versatility in the number of observations available to relate connectivity to streamflow and runoff response (Figures 5.9 and 5.10) and further define the shape of the characteristic curves and any hysteretic tendencies that might exist within them. In this investigation the condition of connectivity and its reverse, dis-connectivity in any individual stream connection was treated as a binary response. As can be observed from any stage discharge relationship, this is an oversimplification. However, for the remote treatment of the large quantity of connections in this project it was a necessity.

Ultimately, streamflow prediction in heterogeneous and seasonally poorly connected systems could benefit most from analyses of connectivity that provide a functional prediction of runoff response timing as well and streamflow. A functional prediction of response timing based on a graph network approach to connectivity dynamics should take a similar form to the volume to



breakthrough discussed by Bracken and Croke (2008). It should incorporate the antecedent connectivity, antecedent storage capacities in the drainage network's inactive elements, and a pre-emptive routing routine to estimate the volume of precipitation required to re-activate inactive gatekeeper elements obstructing flow through the stream network. The accurate prediction of streamflow and runoff response in a heterogeneous drainage basin with dynamic connectivity will require both an account of the presence or absence of connections but also an incorporation of aspects of local function that control the flow through connections themselves.

## CHAPTER 6: CONCLUSIONS

In order to improve understanding of connectivity dynamics in heterogeneous drainage basins, a graph theory based method to quantify hydrological connectivity was proposed. It was used to explore the research questions and satisfy the objectives of this thesis, which were to 1) investigate the dynamics of hydrological connectivity during a typical water year, 2) define the relationship between the contributing stream network and contributing area, 3) investigate how hydrological connectivity influences streamflow, and 4) define how hydrological connectivity influences runoff response to rainfall events. At the Baker Creek Research Basin, hydrological connectivity was found to be highest during the spring freshet but decreased significantly in late May and early June as the stream network was segmented into one component connected to the outlet and many components that were active but disconnected from the outlet. Connectivity could increase due to precipitation inputs in the summer if sufficiently large enough to overcome storage deficits of inactive elements. It was also observed that the contributing area and contributing stream lengths were related by power relationships. A relationship similar to Hack's Law and independent of scale was found to hold for the longest stream supported by a variable contributing area. Connectivity was observed to be positively related to streamflow and runoff response. However, the characteristics of the increases in streamflow and runoff ratio with increased connectivity varied by sub-basin and were strongly influenced by land cover heterogeneity. Differing landscape elements and arrangements affected streamflow and runoff response in different ways. In particular, basin scale connectivity dynamics were driven by

gatekeeper elements which played a defining role in maintaining or disrupting the connectivity of elements lying upstream. The type and placement of gatekeeper elements controlled their storage state and heavily influenced connectivity at larger scales. Gatekeeper function controlled both the presence of and flow through connections throughout the stream network and thus connectivity and streamflow at the basin scale.

The key findings were that connectivity was highly dynamic and that certain aspects of landcover heterogeneity play a strong role in connectivity dynamics and the relationship between connectivity and basin streamflow. The implications of these findings are that accurate prediction of streamflow and runoff response in a heterogeneous drainage basin with dynamic connectivity will require both an account of the presence or absence of connections but also a differentiation of connection type and an incorporation of aspects of local function that control the flow through the connections themselves.

## REFERENCES:

Ali, G. and Roy, A.: Revisiting hydrological sampling strategies for an accurate assessment of hydrologic connectivity in humid temperate systems. *Geography Compass* 3, 350-374, 2009.

Allan, C.J. and. Roulet, N.T.: Runoff Generation in Zero-Order Precambrian Shield Catchments: The stormflow response of a heterogeneous landscape. *Hydrological Processes* 8, 369-388, 1994.

Ambrose, B.: Variable „active’ versus „contributing’ areas or periods: a necessary distinction. *Hydrological Processes* 18, 1149-1155, 2004.

Beven, K. and Wood E.F.: Basin Geomorphology and the Dynamics of Runoff Contributing Areas, *Journal of Hydrology*, 65, 139-158, 1983.

Black, PE. Watershed functions. *Journal of the American Water Resources Association* 33, 1-11, 1997.

Bracken, L. and Croke, J.: The concept of hydrological connectivity and its contribution to understanding runoff-dominated geomorphic systems. *Hydrological Processes* 21, 1749-1763, 2007.

Buttle, J.: Mapping first order controls on streamflow from drainage basins: the T<sup>3</sup> template. *Hydrological Processes* 20, 3415-3422, 2004.

Chartrand, G.: *Introductory Graph Theory*, Dover, New York, 1977.

Chow, V.T., Maidment, D.R., and Mays, L.N.: *Applied Hydrology*, McGraw Hill, Toronto, 1988.

Congalton R.J.: A review of assessing the accuracy of classifications of remotely sensed data. *Remote Sensing of the Environment*, 37, 34-46, 1991.

Dingman S.L.: Effects of permafrost on stream characteristics in the discontinuous permafrost zone of Central Alaska. In *Permafrost: North American Contribution to the Second International Conference*. National Academy of Sciences: Washington, DC; 447-453, 1973.

Dingman, S.L.: *Physical Hydrology*, Waveland Press Inc., Long Grove, Illinois, 2002.

Domenico, P.A. and Schwartz, W.: *Physical and Chemical Hydrogeology*, Wiley, Toronto, 1998.

Ecosystem Classification Group.: Ecological Regions of the Northwest Territories-Taiga Shield. Department of Environment and Natural Resources, Government of the Northwest Territories, Yellowknife, NT, Canada, 2008.

Fang, X., Pomeroy J.W., Westbrook C.J., Guo X., Minke A.G. and Brown T.: Prediction of snowmelt derived streamflow in a wetland dominated prairie basin. *Hydrology and Earth System Science*, 14, 991-1006, 2010.

Goodwin, B.: Is landscape connectivity a dependent or independent variable? *Landscape Ecology* 8, 687-699, 2003.

Granger, R. J. and Hedstrom, N.: Controls on open water evaporation. *Hydrology and Earth Systems Sciences*. 7, 2709-2726, 2010.

Gray, D.M.: Interrelationships of watershed characteristics. *Journal of Geophysical Research* 4, 1215-1233, 1961.

Gray, D. M., Toth, B., Zhao, L., Pomeroy, J. W., Granger, R. J.: Estimating areal snowmelt infiltration into frozen soils. *Hydrological Processes* 15, 3095-3111, 2001.

Gross, J.S., and Yellen, J.: *Graph Theory and Its Applications*, New York, Chapman and Hall/CRC, 2006.

Guan, X.J., Spence, C., and Westbrook, C.J.: Shallow soil moisture – ground thaw interactions and controls: 2. Influences of water and energy fluxes, *Hydrology and Earth System Sciences* 14, 1387-1400, 2010.

Hack, J.T.: Studies of longitudinal profiles in Virginia and Maryland. U.S. Geological Survey Professional Paper, 294-B, 1957.

Heron, R. and Woo, M.K.: Snowmelt computation for a High Arctic site. *Proceedings 35<sup>th</sup> Eastern Snow Conference*, Hanover, New Hampshire, 162-172.

Horst TW.: A simple formula for attenuation of eddy fluxes measured with first order response scalar sensors. *Boundary Layer Meteorology* 94: 517-520, 1997.

James, A. and Roulet, N.: Investigating hydrological connectivity and its association with threshold change in runoff response in a temperate forested watershed. *Hydrological Processes* 21, 3391-3408, 2007.

Jensco, K., McGlynn, B., Gooseff, M., Wondzell, S., Becala, K., and Marshall, L.: Hydrological connectivity between landscapes and streams: Transferring reach- and plot- scale understanding to the catchment scale. *Water Resources Research* 45, 1-16, 2009.

Kaimal, JC, Finnigan JJ. 1994. *Atmospheric Boundary Layer Flows – Their Structure and Measurement*. Oxford University Press. New York, 289 pp.

Kerr, D.E., and Wilson, P.: Preliminary surficial geology studies and mineral exploration consideration in the Yellowknife area, Northwest Territories. Geological Survey of Canada, Current Research 2000-C3, 1-8, 2000.

Kindlmann, P. and Burel, F.: Connectivity measures: a review. *Landscape Ecology* 23, 879-890, 2008.

Kirkby, M, Bracken, L., Reaney, S.: The influence of land use, soils and topography on the delivery of hillslope runoff to channels in SE Spain. *Earth Processes and Landforms* 27 1459-1473, 2002

Kouwen, N.: WATFLOOD/WATROUTE: Hydrological model routing and flow forecasting system, Waterloo, University of Waterloo Department of Civil Engineering, 2010.

Lehmann, P., Hinz, C., McGrath, G., Tromp-van Meerveld, H.J., and McDonnell, J.J.: Rainfall threshold for hillslope outflow: an emergent property of flow pathway connectivity. *Hydrology and Earth System Sciences* 11, 1047-1063, 2007.

Massman, W.J.: A simple method for estimating frequency response corrections for eddy covariance systems. *Agricultural and Forest Meteorology*, 104, 185-198. 2000.

McFeeters, S.K.: The use of normalized difference water index (NDWI) in the delineation of open water features. *International Journal of Remote Sensing*, 7, 1425-1432, 1996.

McNamara, J.P., Kane, D.L., Hinzman, L.D.: An analysis of stream flow hydrology in the Kuparuk river basin, Arctic Alaska: a nested watershed approach. *Journal of Hydrology* 206: 39–57, 1998.

Mielko, C., and Woo M.K.: Snowmelt runoff processes in a headwater lake and its catchment, subarctic Canadian Shield. *Hydrological Processes* 20, 987-1000, 2006.

Quinton, W., Hayashi, M., and Pietroniro, A.: Connectivity and storage functions of channel fens and flat bogs in northern basins. *Hydrological Processes* 17, 3665-3684, 2003.

Quinton, W., and Carey, S.: Towards an energy-based runoff generation theory for tundra landscapes. *Hydrological Processes* 22, 4649-4653, 2008.

Quinton, W.L. and Marsh, P.: A conceptual framework for runoff generation in a permafrost environment. *Hydrological Processes*, 12, 2563-2591, 1999.

Park, J.O.: Vegetation patterns and moisture availability in the Baker Creek Basin, near Yellowknife, NWT, M.Sc. Thesis, University of Alberta, Edmonton, 1979.

Pietroniro, A., Fortin, V., Kouwen, N., Neal, C., Turcotte, R., Davison, B., Versegny, D., Soulis, E. D., Caldwell, R., Evora, N., and Pellerin, P.. Development of the MESH modelling system

for hydrological ensemble forecasting of the Laurentian Great Lakes at the regional scale. *Hydrology and Earth System Science* 11, 1279–1294, 2007.

Pomeroy, J.W., Toth, B., Granger, R.J., Hedstrom, N.R., Essery, R.L.H.: Variation in surface energetics during snowmelt in complex terrain. *Journal of Hydrometeorology*, 4, 702-716, 2003

Pomeroy, J.W., Gray, D.M., Brown, T., Hedstrom, N.R., Quinton, W.L., Granger, R.J., Carey, S.K.: The cold regions hydrological model: a platform for basing process representation and model structure on physical evidence. *Hydrological Processes* 21, 2650–2667, 2007.

Reaney, S.M., Bracken, L.J., Kirkby, M.J.: Use of the connectivity of runoff model to investigate the influence of storm characteristics on runoff generation and connectivity in semi-arid areas. *Hydrological Processes*, 21, 894-906, 2007.

Rigon, R., Rodriguez-Iturbe, I., Maritan, A., Giacometti, A., Tarboton, D.G., and Rinaldo, A.G.: On Hack's law. *Water Resources Research*, 11, 3367-3374, 1996.

Rodriguez-Iturbe, I., and Rinaldo, A.G.: *Fractal River Basins: Chance and Self Organization*. New York, Cambridge University Press, 1997.

Sahimi, M.: *Applications of Percolation Theory*, London, Taylor and Francis, 1984.

Schröder, B.: Pattern, process, and function in landscape ecology and catchment hydrology – how can quantitative landscape ecology support predictions in ungauged basins? *Hydrology and Earth Systems Science*, 10, 967-979, 2006.

Shaw, D.A., Martz, L.W., Pietroniro, A.: The influence of surface water connectivity on runoff volume in the prairie pothole region. *Journal of Hydrology*, in review, 2010.

Spence, C.: Hydrological processes and stream flow in a lake dominated watercourse, *Hydrological Processes* 20, 3665-3681, 2006.

Spence, C.: On the relation between dynamic storage and runoff: A discussion on thresholds, efficiency, and function, *Water Resources Research* 43, 1-11, 2007.

Spence, C.: A paradigm shift in hydrology: Storage thresholds across scales influence catchment runoff generation. *Geography Compass* 4: 819-833, 2010.

Spence, C., Guan, X.J., Phillips, R., Hedstrom, N., Granger, R., and Reid, B.: Storage dynamics and streamflow in a catchment with a variable contributing area. *Hydrological Processes*, 24, 2209– 2221, 2010.

Spence, C. and Woo, M.K.: Hydrology of the subarctic Canadian Shield: Bedrock Upland. *Journal of Hydrology* 262, 111-127, 2002.

Stauffer, D. and Ahorony, A.: *Introduction to Percolation Theory*, London, Taylor and Francis, 1994.

Stichling, W. and Blackwell, S.R.: Drainage area as a hydrologic factor on the glaciated Canadian prairies, IUGG Proceedings, Volume 111, Toronto, Ontario, 12 pp, 1957.

Töyrä J., Pietroniro, A., Martz, L.W. and Prowse, T.D.: A multi-sensor approach to wetland flood monitoring. *Hydrological Processes* 16, 1569-1581, 2010.

Tromp van-Meerveld, H.J. and McDonnell, J.J.: Threshold relations in subsurface stormflow: 2. the fill and spill hypothesis. *Water Resources Research* 42, 1-11, 2006.

Urban, D., and Keitt, T.: Landscape connectivity: a graph-theoretical perspective. *Ecology* 82, 1205-1218, 2001.

Western, A., Blöschl, G., and Grayson, R.: Toward capturing hydrologically significant connectivity in spatial patterns. *Water Resources Research* 37, 83-97, 2001.

Wolfe, S.A.: *Living with Frozen Ground: A Field Guide to Permafrost in Yellowknife*, Miscellaneous Report 64, Geological Survey of Canada, Northwest Territories, 71 pp., 1998.

Woo, M.K. and Mielko, C.: An integrated framework of lake-stream connectivity for a semi-arid, subarctic environment. *Hydrological Processes* 21, 2668-2674, 2007.

Xu, H.: Modification of normalized difference water index to enhance open water features in remotely sensed imagery. *International Journal of Remote Sensing* 14, 3025-3033, 2006



## APPENDIX A: RATING CURVES

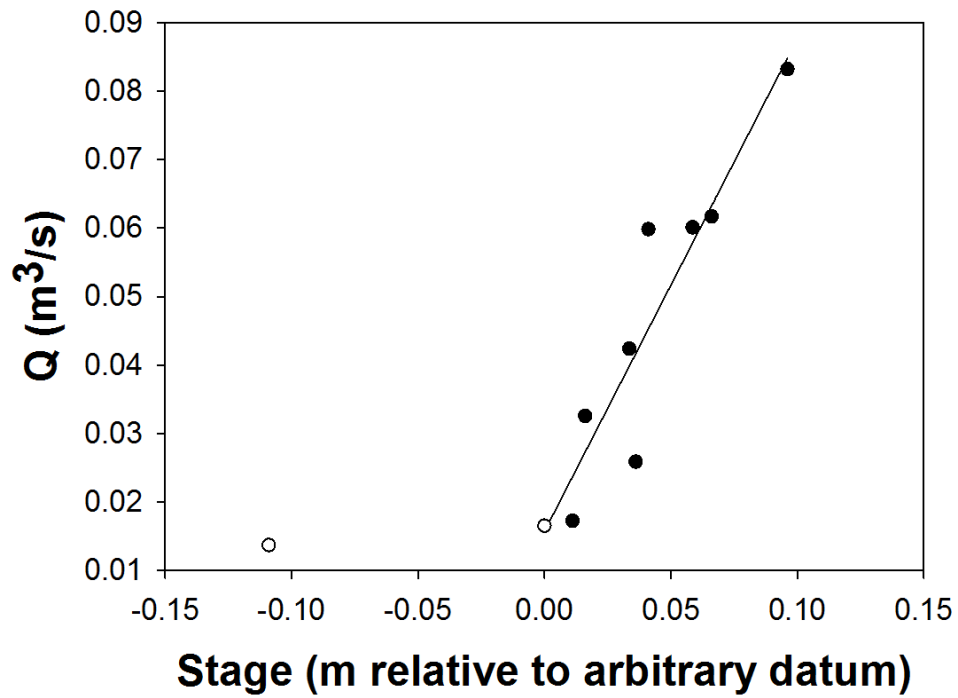


Figure A.1: Trail Lake streamflow (Q) rating curves for stages  $\geq 0$  (level of debris dam) with  $r^2 = 0.87$  and  $Q = 0.0157 + 0.7192 \cdot \text{Stage}$ .

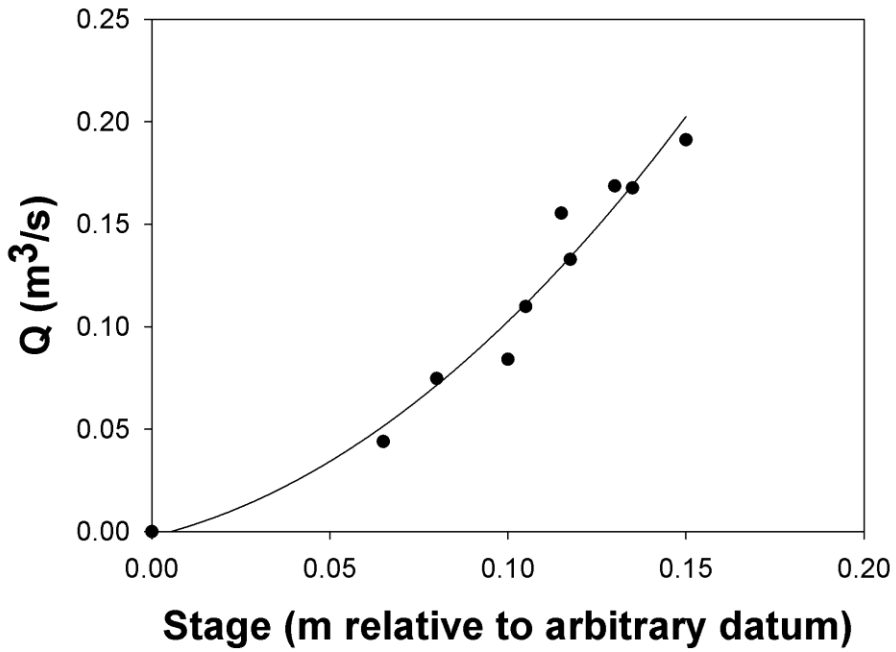


Figure A.2: Eagle Pass Creek streamflow (Q) rating curves for stages  $\geq 0$  (level of earthen dam) with  $r^2 = 0.96$  and  $Q = 6.3234(\text{Stage})^2 + 0.4178(\text{Stage}) - 0.0024$

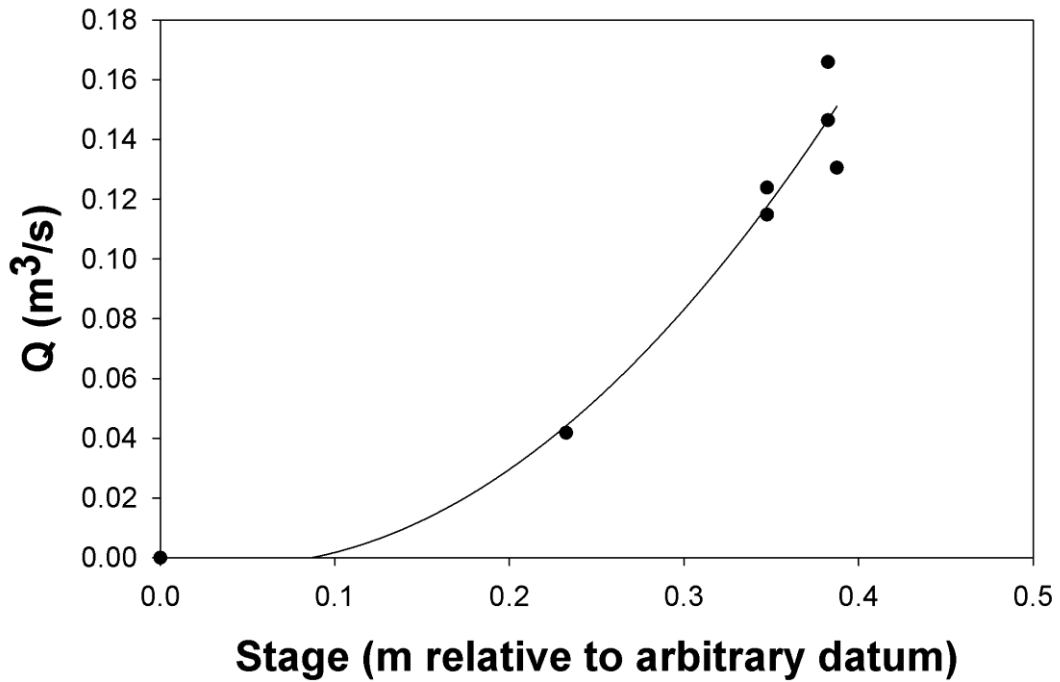


Figure A.3: Baker Creek below Duckfish Lake streamflow (Q) rating curves for stages  $\geq 0$  (level of bedrock sill) with  $r^2 = 0.96$  and  $Q = 1.2861(\text{Stage})^2 + 0.1076(\text{Stage}) - 0.0003$